

Effect of elevated temperature on mechanical and physical properties of high strength concrete modified with graphite nano/micro platelets



Hafiz Waheed Iqbal

Fall 2016-MS Structural Engineering
00000171637

MASTERS IN STRUCTURAL ENGINEERING

MS Thesis Advisor:

Dr. Rao Arsalan Khushnood

**NUST Institute of Civil Engineering (NICE)
School of Civil and Environmental Engineering (SCEE)
National University of Sciences and Technology (NUST)**

Islamabad, Pakistan (2019)

This is to certify that

Thesis titled

**Effect of elevated temperature on mechanical and physical
properties of high strength concrete modified with graphite
nano/micro platelets**

Submitted by

Hafiz Waheed Iqbal

Fall 2016-MS Structural Engineering

00000171637

Has been accepted towards the partial fulfillment

of

the requirements for the award of degree of

Master of Science in Structural Engineering

Dr. Rao Arsalan Khushnood
Assistant Professor

**NUST Institute of Civil Engineering (NICE)
School of Civil and Environmental Engineering (SCEE)
National University of Sciences and Technology (NUST),
Islamabad, Pakistan**

THESIS ACCEPTANCE CERTIFICATE

Certified that final copy of MS thesis written by **Mr. Hafiz Waheed Iqbal**, Registration No. **(00000171637)**, of MS Structure 2016 Batch (NICE) has been vetted by undersigned, found completed in all respects as per NUST Statutes/Regulations, is free of plagiarism, errors, and mistakes and is accepted as partial fulfillment for award of MS/MPhil degree.

Signature _____

Name of Supervisor Dr. Rao Arsalan Khushnood

Date: _____

Signature (HoD) _____

Date: _____

Signature (Dean/Principal) _____

Date: _____

Acknowledgements

First of all, thanks to ALLAH Almighty as with His blessings, His will and His eternal love, I am able to complete my thesis.

I would like to show gratitude towards my family and teachers for their continuous support and love throughout my career. I always found them alongside me while encouraging me in achieving my goals.

In particular, I would like to extend my sincere gratitude for my supervisor Dr. Rao Arsalan Khushnood for his consistent guidance during this whole time. I have been so grateful to have him as a mentor, who responded to my queries so promptly. Thanks to him for the motivation he has given me in my hard times. His positive outlook really inspired me and gave me confidence. I also feel pleased to thank my co-supervisors Dr. Muhammad Usman, Dr. Fawad Ahmad Najam and Dr. Adnan Nawaz for their guidance.

Last but not the least, special thanks to Waqas Lateef Baloch and all my friends as well other faculty persons for putting their time and hard work with me during various stages of the project.

Abstract

Graphite nano/micro platelets (GNMPs) are one of the most promising nano materials because of their pozzolanic reactivity besides the micro-pore filling effect. It is imperative to characterize their behavior under different service conditions. Fire plays vital role in varying condition of concrete structures and properties of concrete change promptly when exposed to higher temperature. Hence, the necessity to characterize properties of GNMPs at elevated temperature becomes important. An experimental program was designed to investigate the properties of high strength concrete (HSC) modified with different percentages of graphite nano/micro platelets (GNMPs) after exposure to elevated temperature. Diversion, restriction and blocking of cracks at nano and micro level, strong bonding with matrix, high surface area and unique carbon-carbon hexagonal plane structure make GNMPs to have excellent mechanical, electrical and thermal properties. Mechanical properties such as compressive strength, tensile strength, stress-strain response, elastic modulus and mass loss of concrete mixtures modified with different percentages of GNMPs have been studied at elevated temperature in 23-800°C range and discussed in detail. Heating rate of 5°C per minute was selected for the cylindrical specimens to reach target temperatures up to 800°C. Scanning electron microscopy (SEM) was used for the study of morphological changes such as crack formation, microstructural damage and the dispersions of GNMPs. Durability properties have been assessed using non-destructive testing technique such as ultrasonic pulse velocity (UPV). Two different types of cooling techniques were used to cool down the heated samples to ambient temperatures. Results showed better retention of mechanical and physical properties of high strength concrete containing GNMPs. Data obtained was utilized to formulate mathematical relationships for expressing mechanical and durability related properties of HSC modified with different percentages of GNMPs as a function of temperature.

Acknowledgements	iv
Abstract	v
List of Figures	viii
List of Tables	x
1 Introduction.....	1
1.1 General.....	1
1.2 Research objectives.....	4
1.3 Research tasks.....	4
1.4 Research significance.....	5
1.5 Thesis outline	5
2 Literature review	6
2.1 General.....	6
2.2 Nanomaterial.....	6
2.3 Carbon-based cementitious nanocomposites	6
2.4 Graphite nano platelets (GNPs)	7
2.4.1 Properties of GNP	8
2.4.2 Applications of GNP	9
2.4.3 Approaches to synthesize nano-graphite platelets	9
2.4.4 Dispersion and characterization of GNMPs.....	11
2.5 High temperature testing methods based on heating and loading regimes	12
2.6 Rapid cooling/Quenching method	13
2.7 High Strength Concrete (HSC)	14
2.8 Silica Fume	14
2.8.1 Advantages of using silica fume	14
2.8.2 Reaction mechanism of silica fume	15
2.8.3 Effect of silica fume on the hardened properties of concrete.....	15
2.9 Effect of Elevated Temperatures on HSC.....	17
2.9.1 Introduction.....	17
2.9.2 Microstructural and Chemical properties.....	17
2.9.3 Physical properties	18
2.9.4 Mechanical properties	20
2.10 Effect of GNPs on Cementitious composites and Concrete.....	23
2.10.1 GNPs effect on mechanical and thermal properties	23
3 Experimental Program	26
3.1 General.....	26
3.2 Materials	26
3.3 Mix proportions and preparation of specimen	30

3.4	Target temperatures for test methods	31
3.5	Test equipment and procedure	31
3.5.1	Compressive strength test	32
3.5.2	Splitting tensile strength.....	33
3.5.3	Stress-strain curve	33
3.5.4	Elastic modulus	33
3.5.5	Mass loss	34
3.5.6	Non-Destructive Testing	34
4	Results and discussion	35
4.1	Visual assessment and spalling of concrete	35
4.2	Compressive strength.....	38
4.2.1	Compressive strength tests for residual test condition	38
4.2.2	Compressive strength for rapid cooling/quenching method	41
4.3	Tensile strength.....	43
4.3.1	Residual tensile strength	43
4.3.2	Tensile strength for rapid cooling/quenching method	45
4.4	Stress-strain response.....	46
4.4.1	Residual stress strain response	46
4.4.2	Stress strain response for rapid cooling/quenching method.....	48
4.5	Modulus of elasticity.....	49
4.5.1	Residual modulus of elasticity	50
4.5.2	Modulus of elasticity for rapid cooling/quenching method	51
4.6	Ultrasonic pulse velocity test	53
4.6.1	Residual Ultrasonic pulse velocity.....	53
4.6.2	Ultrasonic pulse velocity for rapid cooling/quenching method	54
4.7	Mass loss.....	54
4.7.1	Residual Mass loss	55
4.7.2	Mass loss for rapid cooling/quenching method	56
4.8	Mathematical relationships	56
5	Conclusions.....	59
6	References.....	61

List of Figures

FIGURE 1: STRUCTURES OF SINGLE-WALLED CARBON NANO TUBES (SWCNT) AND MULTI-WALLED CARBON NANO TUBES (MWCNT) [33]	6
FIGURE 2 : STRUCTURE OF GRAPHENE SHEET SHOWING THE SP ² HYBRIDIZED CARBON ATOMS [46].....	7
FIGURE 3 : SCHEMATIC ILLUSTRATION OF GNP PRODUCTION (VICULIS) [33].	8
FIGURE 4 : SCHEME OF THE GRAPHITE STRUCTURE MODIFICATION DURING GRAPHITE INTERCALATION METHOD [48].....	10
FIGURE 5 : SCHEMATIC ILLUSTRATION OF GNP PRODUCTION [VICULIS] [22]	11
FIGURE 6 : UV-VIS SPECTROSCOPY OF GUM ARABIC WITH GRAPHITE NANO /MICRO PLATELETS.....	12
FIGURE 7 : LOADING AND HEATING CONDITIONS FOR TEST METHODS A) STRESSED B) UNSTRESSED C) RESIDUAL [14].....	13
FIGURE 8 : SEM OF CONCRETE SAMPLE AFTER EXPOSURE TO 800°C [69].	18
FIGURE 9 : SURFACE CRACKING OF CONCRETE SAMPLES AFTER EXPOSURE TO HIGH TEMPERATURES [12].	19
FIGURE 10 : PARTICLE SIZE ANALYSIS AND FESEM OF GRAPHITE.....	29
FIGURE 11 : EDS OF GRAPHITE	30
FIGURE 12 : ELECTRIC FURNACE FOR HEATING THE SAMPLES TO TARGETED TEMPERATURES.....	31
FIGURE 13 : UNIVERSAL TESTING MACHINE FOR MECHANICAL TESTING	32
FIGURE 14 : COLOR CHANGE, CRACKING AND SPALLING VISUALS OF REFERENCE AND MODIFIED HSC WITH NANO/MICRO GRAPHITE PLATELETS AT AMBIENT AND ELEVATED TEMPERATURE CONDITIONS (RESIDUAL TEST CONDITION).....	37
FIGURE 15 : COLOR CHANGE, CRACKING AND SPALLING VISUALS OF REFERENCE AND MODIFIED HSC WITH NANO/MICRO GRAPHITE PLATELETS AT AMBIENT AND ELEVATED TEMPERATURE CONDITIONS (RAPID COOLING/QUENCHING TEST CONDITION)	38
FIGURE 16 : VARIATION IN ABSOLUTE COMPRESSIVE STRENGTH OF HSC AND NANO/MICRO GRAPHITE PLATELETS MODIFIED HSC AT AMBIENT AND ELEVATED TEMPERATURES	39
FIGURE 17 : VARIATION IN RELATIVE COMPRESSIVE STRENGTH OF HSC AND NANO/MICRO GRAPHITE PLATELETS MODIFIED HSC AT AMBIENT AND ELEVATED TEMPERATURES	40
FIGURE 18 : MICROGRAPH OF 0.3GNMPs CONCRETE AFTER BEING EXPOSED TO ELEVATED TEMPERATURE OF 400°C	40
FIGURE 19 : VARIATION IN RELATIVE COMPRESSIVE STRENGTH OF HSC AND NANO/MICRO GRAPHITE PLATELETS MODIFIED HSC AT AMBIENT AND ELEVATED TEMPERATURES (RAPID COOLING/QUENCHING TEST METHOD)41	
FIGURE 20: VARIATION IN RESIDUAL TENSILE STRENGTH OF HSC AND NANO/MICRO GRAPHITE PLATELETS MODIFIED HSC AT AMBIENT AND ELEVATED TEMPERATURES	44
FIGURE 21: VARIATION IN RELATIVE RESIDUAL TENSILE STRENGTH OF HSC AND NANO/MICRO GRAPHITE PLATELETS MODIFIED HSC AT AMBIENT AND ELEVATED TEMPERATURES	44
FIGURE 22 : VARIATION IN ABSOLUTE TENSILE STRENGTH OF HSC AND NANO/MICRO GRAPHITE PLATELETS MODIFIED HSC AT AMBIENT AND ELEVATED TEMPERATURES (RAPID COOLING/QUENCHING TEST METHOD)45	
FIGURE 23 : VARIATION IN RELATIVE TENSILE STRENGTH OF HSC AND NANO/MICRO GRAPHITE PLATELETS MODIFIED HSC AT AMBIENT AND ELEVATED TEMPERATURES (RAPID COOLING/QUENCHING TEST METHOD)46	
FIGURE 24 : RESIDUAL STRESS-STRAIN RESPONSE AT AMBIENT AND ELEVATED TARGETED TEMPERATURES OF ...	48
FIGURE 25 : STRESS-STRAIN RESPONSE AT AMBIENT AND ELEVATED TARGETED TEMPERATURE OF ANALYZED....	49
FIGURE 26 : VARIATION IN ABSOLUTE RESIDUAL MODULUS OF ELASTICITY OF HSC AND NANO/MICRO GRAPHITE PLATELETS MODIFIED HSC AT AMBIENT AND ELEVATED TEMPERATURES	50
FIGURE 27 : VARIATION IN RELATIVE RESIDUAL MODULUS OF ELASTICITY OF HSC AND NANO/MICRO GRAPHITE PLATELETS MODIFIED HSC AT AMBIENT AND ELEVATED TEMPERATURES	51
FIGURE 28 : VARIATION IN RELATIVE MODULUS OF ELASTICITY OF HSC AND NANO/MICRO GRAPHITE PLATELETS MODIFIED HSC AT AMBIENT AND ELEVATED TEMPERATURES (FAST COOLING/QUENCHING METHOD).....	52
FIGURE29: VARIATION IN RELATIVE MODULUS OF ELASTICITY OF HSC AND NANO/MICRO GRAPHITE PLATELETS MODIFIED HSC AT AMBIENT AND ELEVATED TEMPERATURES (FAST COOLING/QUENCHING METHOD).....	52
FIGURE 30: VARIATION IN RESIDUAL UPV OF HSC AND NANO/MICRO GRAPHITE PLATELETS MODIFIED HSC AT AMBIENT AND ELEVATED TEMPERATURES	53
FIGURE 31: VARIATION IN UPV OF HSC AND NANO/MICRO GRAPHITE PLATELETS MODIFIED HSC AT AMBIENT AND ELEVATED TEMPERATURES (RAPID COOLING/QUENCHING METHOD)	54
FIGURE 32 : RESIDUAL RELATIVE DECREASE IN MASS OF HSC AND NANO/MICRO GRAPHITE PLATELETS MODIFIED HSC AT AMBIENT AND ELEVATED TEMPERATURES.....	55

FIGURE 33 : RELATIVE DECREASE IN MASS OF HSC AND NANO/MICRO GRAPHITE PLATELETS MODIFIED HSC AT AMBIENT AND ELEVATED TEMPERATURES (RAPID COOLING/QUENCHING METHOD) 56

List of Tables

TABLE 1 : COMPARISON BETWEEN GNP & CNT [27].....	9
TABLE 2. PHYSICAL AND CHEMICAL PROPERTIES OF CONCRETE.....	27
TABLE 3. PHYSICAL PROPERTIES OF FINE AND COARSE AGGREGATES.....	27
TABLE 4. ELEMENTAL ELEMENTS OF RAW GRAPHITE	28
TABLE 5. ELEMENTAL COMPOSITION OF GUM ARABIC.....	29
TABLE 6. DETAIL OF MIXTURE PROPORTIONS AND STRENGTH PROGRESSION.....	30
TABLE 7 : HIGH TEMPERATURE MATERIAL PROPERTY RELATIONS FOR HSC AND NANO/MICRO GRAPHITE MODIFIED HSC MIXTURES (RESIDUAL TEST CONDITION).....	57
TABLE 8 : HIGH TEMPERATURE MATERIAL PROPERTY RELATIONS FOR HSC AND NANO/MICRO MODIFIED HSC MIXTURES (RAPID COOLING METHOD/QUENCHING METHOD).....	58

1 Introduction

1.1 General

Concrete is regarded as one of the most broadly used construction material in world because of the fact that it has large number of resources, high adaptability and matured process for production. With appropriate combination of cement, additional cementitious components and less water to cement ratio, different types of concrete are produced for different purposes. For instance, steel fiber reinforcement is used to enhance tensile strength and to bridge the micro cracks but it increases the cost, self-weight and is also ineffective in delaying micro cracks due to large spacing and less interlocking [1–3]. Most of the time the concrete structures become progressively worse when some challenging environments are faced. Moreover, they also require repairs before their service life is ended which are very costly.

A good concrete material should have two criteria; i.e. it should be good in its fresh and hardened state. Concrete should be consistent and cohesive. It must be consistent to such a limit that we can compact it without applying excessive effort, and also it must be not that much cohesive to produce segregation which will reduce the homogeneity of concrete. For a concrete material to be efficient in hardened state, it must have durability and compressive strength [4,5].

In today's world concrete with higher strength and higher performance is being used and for its production, the ratio of water to binder should be reduced and binder content should be high. To achieve lower water to binder ratio, super plasticizers are used in the concrete. Also, to achieve low porosity and permeability different types of cementitious materials can also be added in addition with concrete. Silica fume is added in concrete mixtures which cause lower porosity and permeability. It is one of the most popular pozzolan because their oxides (SiO_2) reaction consumes calcium hydroxides, which are products of hydration of ordinary Portland cement. Pozzolanic reactions results are the lower heat release, lime consumption, strength development and smaller pore size distribution [6].

During fire or near furnaces and reactors, concrete is being exposed to elevated temperature [7]. These exposures can result into decrement of mechanical properties like elastic modulus, strength and stability of volume which leads to structural failures. For determination of load

carrying capacity and for re-establishing of structures which are damaged from fire, it is important to study properties retained after exposure to elevated temperature [8]. Exposure of specimens to heat can considerably change the physical structure and composition of concrete. Above 110°C temperature, significant amount of water which is chemically bonded release through calcium silicate hydrate (CSH) gel [9]. Internal stresses are increased and micro cracks are also produced from 300°C due to expansion of aggregates. Calcium hydroxide (CH) is an important product of hydration reaction is also dissociated at 530°C which can result into the shrinkage of concrete. Cracking and crumbling of concrete are occurred when CaO is turned into calcium hydroxide (CH). Surface cracking and spalling are visible effects of high temperature [10]. This exposure may also cause some color changes. Above 500°C, the transitions due to high temperatures are more noticeable. The changes which concrete experiences on this temperature level are mostly considered irrevocable [11]. Above 600°C, CSH gel, which gives strength to the cement paste also decomposes. With further increase of temperature at 800°C, concrete usually break down. Moreover, some other minerals which are present in the cement paste are converted into the glass phase [8]. This results in changes of the microstructure, strength degradation and durability of concrete [12].

In order to ensure a safe structural fire design which involves HSC, it is also necessary to know about the fundamental behavior of HSC at higher temperatures as it has many benefits and increased use in structures [6]. In the past few decades, supplementary cementitious materials (SCMs) like ground granulated blast furnace slag (GGBFS), silica fume (SF) and fly ash (FA) have been extensively studied to develop hybrid concrete systems. These materials improve interfacial transition zones (ITZ) between mortar and aggregates and help attain dense microstructures, which is reflected by enhanced mechanical properties. However, these densely packed matrices behave contrarily and spall if exposed to elevated temperatures [13]. Spalling occurs due to the sudden cracking in matrix owing to the lack of dissipation of pore pressure [14], development of thermal inertia [15] or concentration of thermal stresses [16]. Behnood and Masoud [17] studied the use of polypropylene fibers (PP) to mitigate spalling. PP fibers being thermally unstable, fuse at around 200°C and provide pockets of space for vapor pressure to dissipate. However, the presence of these pores in turn causes durability issues [18]. Use of fibers such as steel [19] and basalt [20] to incapture cracking have also been explored. These fibers bridge across the cracks by providing anchorage and help to retain the effective load bearing area. However, issues arise with the proper bonding of these fibers in cement matrix [21] and the overall cost [22]. The cementitious materials are usually quasi-brittle, thus are

sensitive to cracking and contain no functional characteristics. Nanotechnology is being introduced in the cementitious materials to resolve the aforementioned issues. In recent years, micro and nano materials have gained considerable attention in material field. Expectations, visions and abilities to control the world of material has changed because of nano technology [23,24]. The nano-materials specifically the carbonaceous nano-inerts like carbon nanotubes (CNTs), carbon nano-fibers (CNFs), and graphite nano-platelets (GNPs) have shown the capacity to improve the mechanical, functional and durability properties of the cementitious materials at ambient conditions [25–27]. Waqas et. al [25,28] has reported the use of multiwalled carbon nanotubes (MWCNTs) to develop fire enduring concrete. The authors suggested that the use of these nano-scale reinforcements not only catered for thermal cracking but also reduced the thermal inertia. The reduction of thermal inertia and uniform scattering of thermal stresses was because of the highly thermal conductive nature of the nanotubes. The field of materials and construction will surely be affected by these developments. Many other research studies also described the capacity of nano carbon materials in the enhancement of cementitious materials like carbon nano tubes, carbon nano fibers and carbon black [25,29]. Carbon Nano fibers (CNF), Carbon Nano tube (CNT) and Graphite Nano platelets (GNPs) are being used to provide nano scale reinforcement for improvement of thermal properties and to enhance cracking resistance of these materials at ambient conditions [26,27,30]. Though a lot of research is available on CNTs and CNFs and the fire behavior of the cementing matrices containing these nano-materials. However, the study on graphite nano-platelets (GNPs) in conjunction with cement matrices exposed to elevated temperature is limited in technical literature.

Further research is being done on the modification of cementitious composites by graphite nano platelets (GNPs) [27]. These GNPs comprise of small sacks of graphene which have the thickness of 0.35-100 nm. Graphene comprises of hexagonal plane made of single carbon-carbon layer and is named as “sub structure unit”. Hence, the structure of GNPs consists of a net like made up of multilayer carbon-carbon hexagonal plane and graphene contains only one layer of carbon atoms and is a special case of GNPs. As a result, the properties of GNPs are regarded as close to graphene. From the past few years, these GNPs are getting more attention in different fields. Different researches have shown that hardness of graphite sheet of single layer to be higher than 100 GPa which is harder than that of diamond [31]. Hence, the performance against abrasion resistance of cement-based composites will be automatically enhanced by the improvement of hardness. So, the composites which are filled with GNPs are

found to have good abrasion resistance performance [32]. Generally, GNPs prepared by intercalated graphite either with acid treatment or with metal ions and then exfoliated by thermal treatment to obtain GNPs [33,34]. Like CNTs, GNPs possess excellent thermal as well as electrical conductivity with enhanced mechanical properties [35,36].

Compared with CNTs (8\$/gram), GNPs (2\$/kg) have lower unit cost and also free from entanglement problem [22]. Blocking and diversion of cracks due to plates feature and delaying of cracks initiation due to bridging effect make GNPs a material having excellent mechanical and thermal properties [22,37,38]. GNPs can be an excellent alternative for the expensive carbon nano tubes.

Material properties of these GNMPs have been explored in some studies and some specifications have been updated at ambient temperatures. There is no significant information available on elevated temperature properties of these nano/micro-reinforced high strength concrete. For predicting the elevated temperature properties there is a requirement for an elaborative experimental data and mathematical models.

1.2 Research objectives

- To study the effect of graphite nano/micro platelets on mechanical properties of high strength concretes subjected to high temperature.
- To study the effect of different cooling methods on mechanical properties of high strength concretes exposed to high temperature.
- To analyze failure pattern of high strength concrete modified with graphite nano/micro platelets subjected to elevated temperature.
- To carry out non-destructive testing (NDT) of the analyzed formulation.
- Development of mathematical relationships for expressing material properties as a function of temperature.

1.3 Research tasks

To accomplish research objectives following tasks were performed.

- Literature review.
- Test set up which includes furnace, splitting tensile test assembly, protective steel assembly.
- Perform tests on high strength concrete samples exposed to elevated temperature.
- Evaluate and analyze experimental results.
- Conclusions and recommendations.

1.4 Research significance

With the envisaged structural applications of nano-modified cementitious matrices, it is imperative to characterize their response for varied conditions. Fire is regarded as harmful hazards from which structures are threatened with during the service life. Hence, the requirement to characterize the mechanical and material behavior of nano-modified matrices at high temperatures becomes significant. The ultrafine particles of nano material act as filler agent and lead to reduction of micro pores and produce a compact concrete which brings about the suspicion about spalling of such concrete at elevated temperature [39,40].

Limited research work is being implemented to observe the behavior of graphite nano/micro platelets (GNMPs) in concrete at ambient temperatures and there is no reliable data available on higher temperature properties of these nano/micro reinforced high strength concrete. For predicting the elevated temperature properties, an elaborative experimental data and mathematical models are required. This study provides mechanical, physical and micro structural properties of high strength concrete modified with various proportions of GNMPs up to the required targeted temperature of 800°C, reflected in literature as ambient to replicate the fire [41,42].

1.5 Thesis outline

The research executed to achieve the mentioned objectives is presented in five chapters.

In chapter 1, effect of fire on high strength concrete, nano/micro material, research objectives and research significance are being discussed.

Chapter 2 describes literature review in detail and about properties of GNMPs in general and when used in cementitious matrices has been provided. Elevated temperature response of HSC and effect of GNMPs at ambient temperature have been discussed in detail, in addition to that cooling methods for heat treated samples are discussed.

Chapter 3 deals with the test setup. It explains which types of equipment are used to evaluate mechanical properties. Furthermore, it presents an overview of the test procedure which describes the ways and methods to determine mechanical properties.

Chapter 4 provides evaluation, analysis and discussion for results of material property tests. Further simple linear empirical high temperature relationships of modified mixes have also been presented.

Chapter 5 provides detailed conclusions

2 Literature review

2.1 General

Introduction about graphite nano/micro platelets, their production and usage in cementitious matrices has been presented in that chapter. Properties of GNMPs at ambient temperature have been discussed. Literature on silica fume and high strength concrete properties at elevated temperature has been discussed.

2.2 Nanomaterial

Nano materials should have at least one dimension in nanometer. Nano materials show different physical and chemical properties than macro-scale material because of change in crystal and surface electronic structure [43].

2.3 Carbon-based cementitious nanocomposites

Studies on carbon-based cementitious nano composites started back in 1990's. Carbon nano tube (CNT) and carbon black (CB) were the two-carbon based nano-particles that were used at that time. CNT has two types, one is single walled carbon nano tube (SWCNT) having diameter of 0.75-3nm and length of 1-50um, other is multi walled carbon nano tube (MWCNT) having diameter of 2-30nm and length of 0.1-50um [44]. SWCNT has only one layer of graphene and MWCNT has multiple layers of graphene (single layer of two-dimensional carbon atoms bonded to form hexagonal lattice is called graphene) [45].

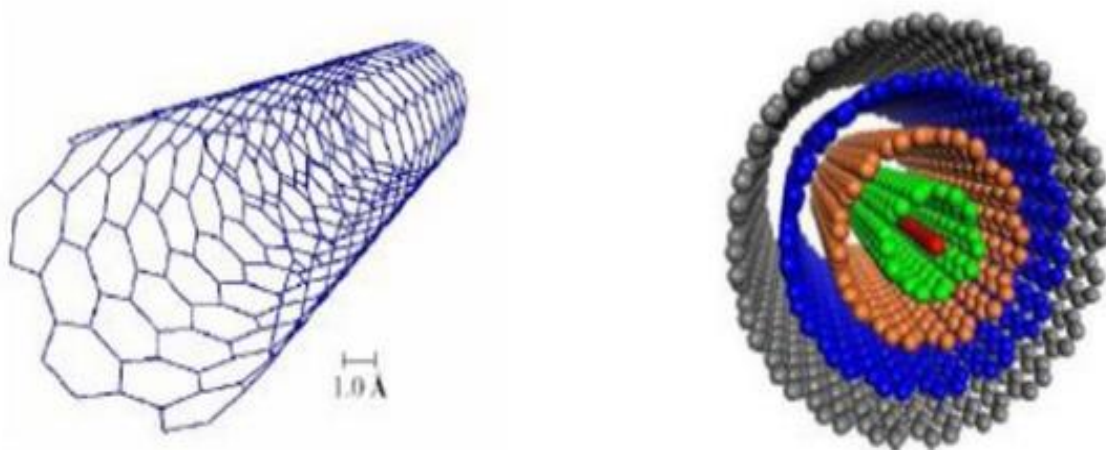


Figure 1: Structures of single-walled carbon nano tubes (SWCNT) and multi-walled carbon nano tubes (MWCNT) [33]

2.4 Graphite nano platelets (GNPs)

Graphite nano platelet (GNP) is a carbon-based nano-material that is obtained from graphite. GNP has two-dimensional platelet structure composed of graphene layers having thickness in nanometer and diameter in the range of submicron to 100 μ m. Because of higher aspect ratio and larger surface area, these nano platelets show good mechanical properties and also make conductive networks in composite materials. Natural graphite consists of parallel graphene layers shown in Figure 2 [46]. GNPs can be obtained by separating these graphene layers with the help of intercalation and exfoliation shown in Figure 3 [33].

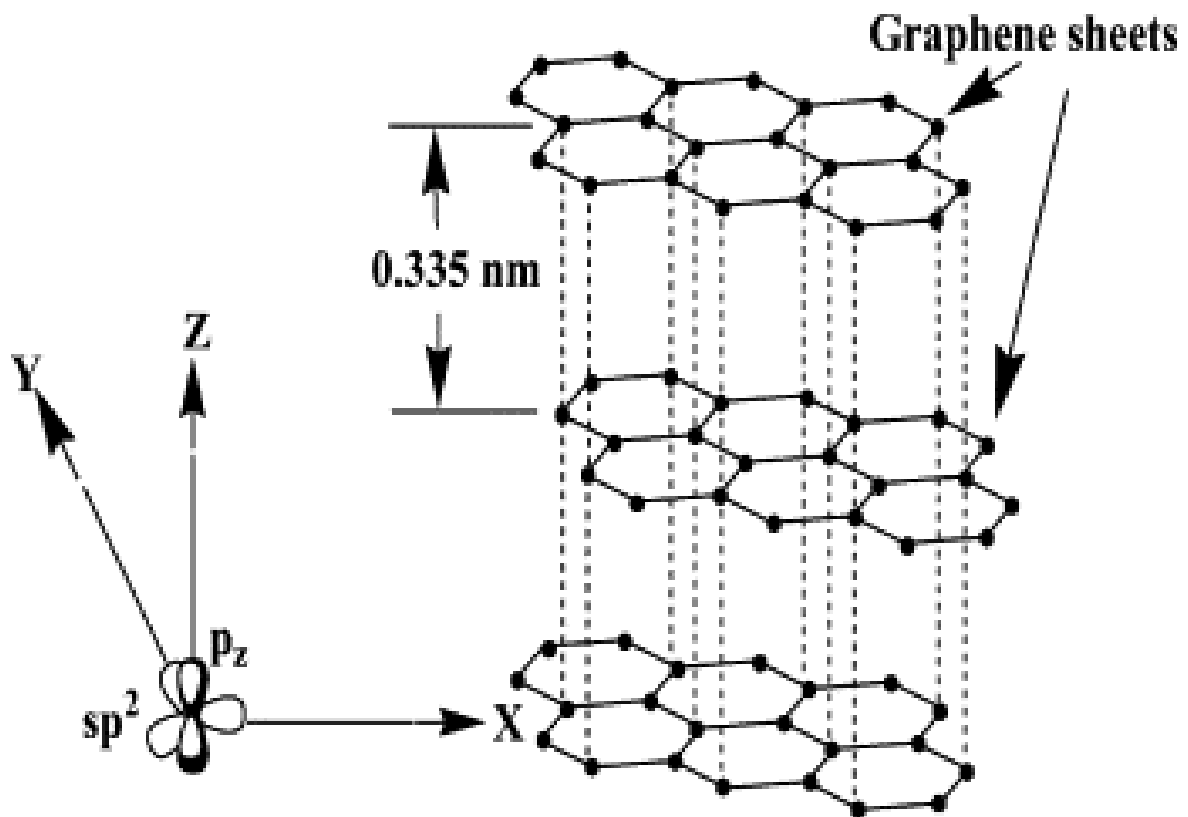


Figure 2 : Structure of graphene sheet showing the sp^2 hybridized carbon atoms [46]

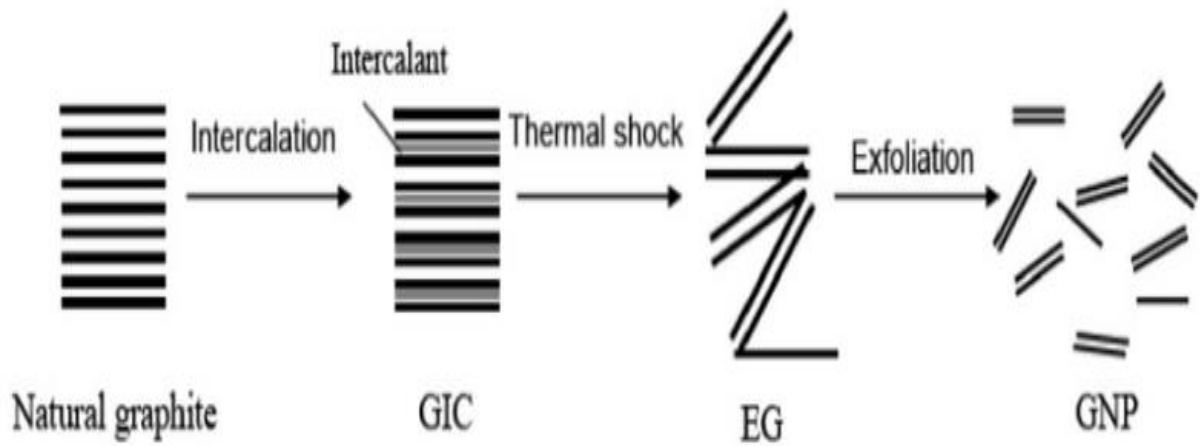


Figure 3 : Schematic illustration of GNP production (Viculis) [33].

2.4.1 Properties of GNP

Due to anisotropic feature of graphite, GNPs have good electrical and mechanical properties along the basal plane. Table 1 shows important properties of GNP and carbon nano tube (CNT). GNPs have good mechanical properties as its elastic modulus is comparable to that of CNT. Entanglement problem is very common in CNT and lot of efforts are required to separate the CNT for homogeneous mixture but due to the platelets feature, GNP is usually free from agglomeration [13]. Furthermore, CNTs are very expensive as MWCNTs price is \$8/g and SWCNTs price is \$170/g, while GNPs price is only \$2/kg [19]. GNP has different electrical properties than carbon black (CB). CB are ball shaped nano particles having aspect ratio 1. Due to ball shape, their conductive path is construct by only points connection, hence possess a higher threshold value in the range of 3-15% for different mixes [22]. Due to higher aspect ratio, GNPs have one order lower percolation value than CB [22]. Price of CB and GNP is same but higher percolation threshold means higher cost and higher energy is required for dispersion. In respect of the above-mentioned important properties, GNP are regarded substitute for the traditional fillers, such as CNT and CB for composite materials [27].

Table 1 : Comparison between GNP & CNT [27]

Property	Unit	GNP	CNT
Elastic modulus	TPa	1 (in-plane)	~1 for SWNT, ~0.3-1 for MWNT
Strength	GPa	~10-20	50-500 for SWNT, 10-60 for MWNT
Resistivity	$\mu\Omega\text{cm}$	50 (in-plane)	~5-50
Dimensions		Diameter: 1-20 μm Thickness: ~30nm	Diameter: 0.75~3nm for SWNTs, 2~30nm for MWNTs. Length: 1~50 μm for SWNTs, 0.1~50 μm for MWNTs
Surface area	m^2/g	~2630	>400
Aspect ratio	-	50-300	~500

2.4.2 Applications of GNP

GNP has many important properties like high thermal and electrical conductivity, higher aspect ratio and higher surface area and because of these properties it is considered as good nano filler. Graphitic filler composites are technical parts of many applications like Li-ion batteries, flame-retardant materials, mechanically stable materials, sensors and solar cells [47].

2.4.3 Approaches to synthesize nano-graphite platelets

GNPs can be synthesized by four methods.

1. Chemical vapor deposition

2. Arc discharge method
3. Mechanical milling
4. Graphite Intercalation

Graphite intercalation method is widely used and is discussed below in detail.

2.4.3.1 Graphite Intercalation method

STEP1

Force is needed to separate the natural graphite layers. A chemical is placed in graphite layers which produce the required force for separation by releasing heat or high amount of gas. The product of this step is called graphite intercalated compound (GIC).

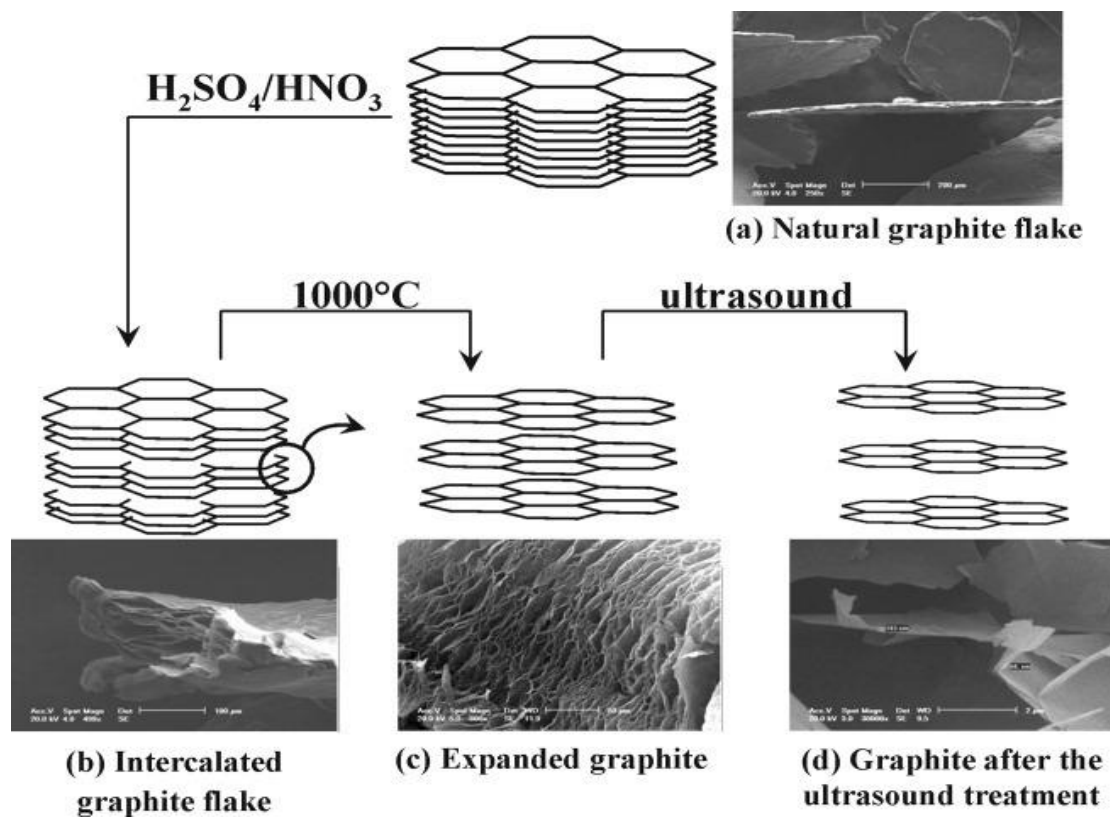


Figure 4 : Scheme of the graphite structure modification during graphite intercalation method [48]

STEP2

Rapid heating of graphite intercalated compound to above 1000°C for 20-30 seconds generates gases like SO₂ and H₂O and expand the GIC to form expanded graphite (EG).

STEP3

In the last step, with the help of ultra-sonification expanded graphite breaks down to form GNP. The process is called exfoliation [48]. The whole process is illustrated in Figure 4.

The whole process can also be represented in Figure 5.

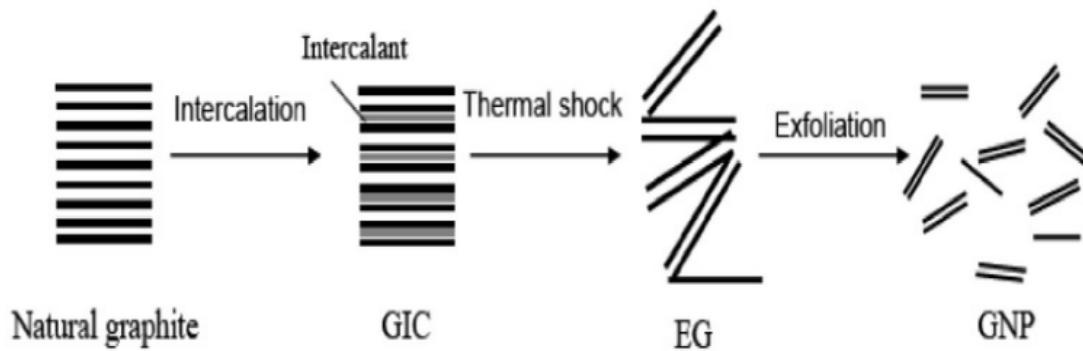


Figure 5 : Schematic illustration of GNP production [Viculis] [22]

2.4.4 Dispersion and characterization of GNMPs

Limited research has been established to study graphite nano/micro platelets (GNMPs) behavior in concrete at ambient temperatures. Various researchers have used different percentages of GNMPs in composites and ultra-high-performance concrete [22,23,27,32,35,43,49]. From previous research, it is concluded that for mechanical properties enhancement, optimum dosage of GNPs is up to 0.5% of weight of cement.

Because of Van der Waals forces, nano/micro platelets of graphite get closely packed and did not disperse into the cementitious matrix. Thus for homogeneous dispersion of GNMPs, a chemical or mineral surfactant aided with mechanical sonication is usually adopted [23,32,38,43,50–52]. In this study, Acacia gum (AG) also called Gum Arabic (GA) was used as surfactant. It weakens the van der waals forces and helps to disperse nano particles as indicated by Waqas et al [25]. GNMPs were diffused by using the surfactant-ultrasonic

technique. Prior to the use of sonication, ultraviolet-visible (UV-Vis) spectroscopy was implied to identify the absorbance values of prepared aqueous dispersions at 500 nanometer (nm) wavelength which remains least affected at the ambient settings [25]. Optimum surfactant to GNMPs ratio was explored via successive dispersions of GNMPs to GA suspensions varying from 0.2 to 1 at the constant interval. Results revealed that surfactant to GNMPs ratio of 0.6:1 is optimum to attain homogeneous suspensions aided with mechanical sonication of 45 minutes, as given in Figure 6.

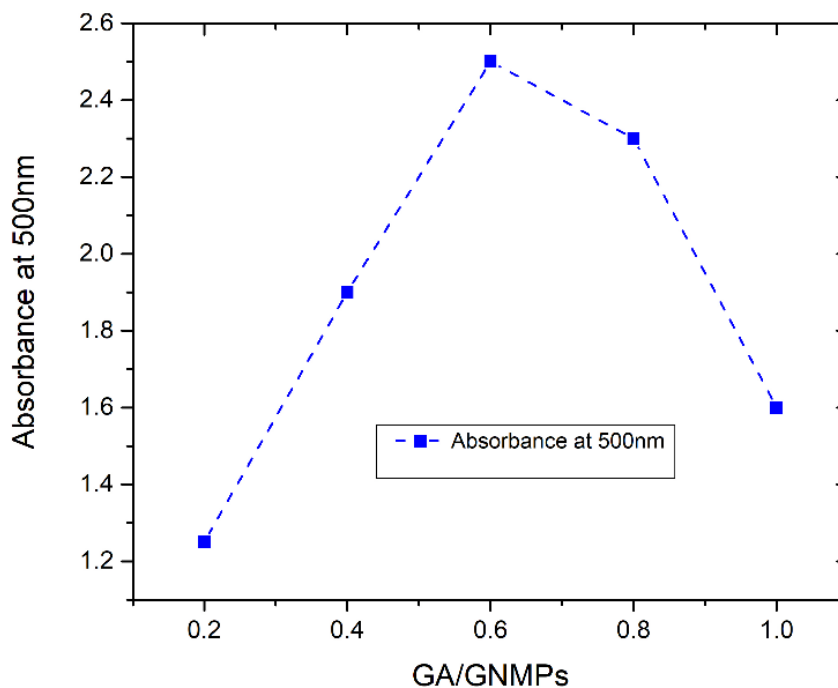


Figure 6 : UV-Vis Spectroscopy of Gum Arabic with Graphite nano /micro platelets.

2.5 High temperature testing methods based on heating and loading regimes

There are three different testing methods available for heat treatment and testing samples which are named as stressed, unstressed and residual. In stressed condition, specimen is loaded to 40% of ultimate strength in pre-heating stage. The sample is then heat treated to required temperature in a recommended ramp time and then temperature is kept constant for suitable time to accomplish thermal steady state. Then further load is applied till sample failure. Schematically it is shown in Figure 7(a). This condition accomplishes actual life fire action. It

is a complex system and special laboratories are established to study fire properties of members under this condition.

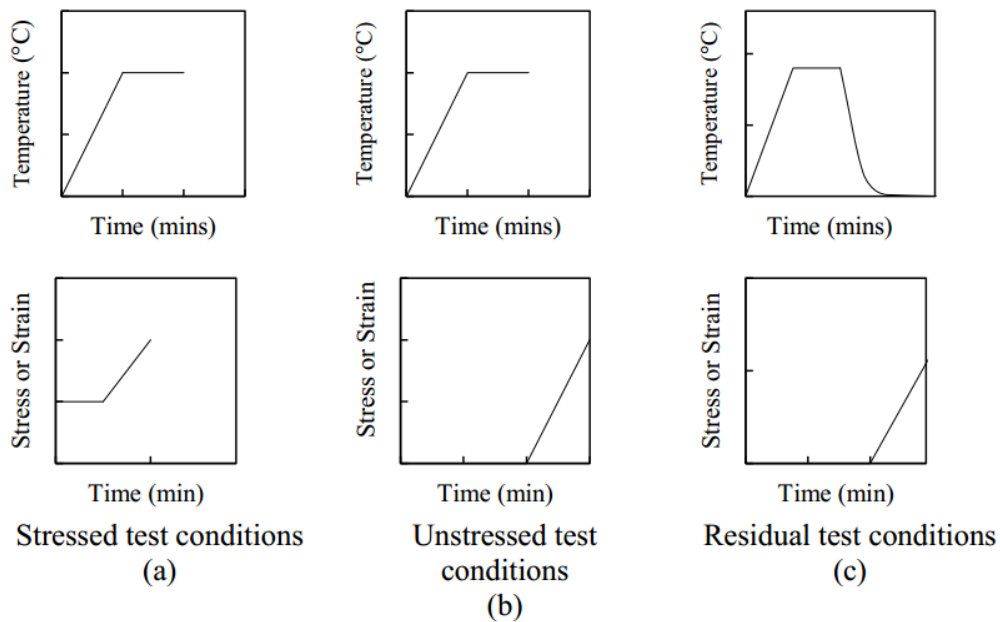


Figure 7 : Loading and heating Conditions for test methods a) stressed b) unstressed c) residual [14]

In unstressed situation, the sample is not subjected to pre-loading. Sample is heated up to target temperature and then held constant for some time at that temperature to attain thermal steady state. Then the sample is tested without any heat loss by covering it with thermal jacket insulation. Results obtained are different from stressed conditions but they give reasonably exact idea about how structure will perform under actual fire condition. Schematic illustration is shown in Figure 7(b).

In residual situation, specimen is heat treated under thermal steady conditions and then sample is cooled down to room temperature. Sample is then loaded till failure. The loading and heating regimes are shown in Figure 7(c). This condition is least accurate but it is easy and simple in execution and due to that reason, most of research associated to high temperatures is established on this method.

2.6 Rapid cooling/Quenching method

After the exposure of specimens to elevated temperature, method of cooling of these specimens to room temperature plays vital impact on strength degradation. Previous research indicate that rapid/fast cooling /quenching technique results in greater compressive strength degradation as

compared to normal cooling by air also called residual test method because of wider cracks formation in rapid/fast cooling technique [53]. After exposure to high temperature, samples were water sprayed for fast cooling [54,55]. Uniform spraying was accomplished by rotating the specimen in front of tap nozzle for 5 minutes [55,56]. Then specimen was allowed to cool down completely to ambient temperature.

2.7 High Strength Concrete (HSC)

HSC is a type of high-performance concrete (HPC), commonly having a compressive strength of 40 MPa or more. For high strength concrete (HSC) production; quality control and greater research is required as compared to conventional concrete [57].

In today's world, concrete with high strength is used and for its production, the ratio of water to binder are reduced and super plasticizers are used in the concrete for that purpose. Also, to achieve low porosity and permeability, different types of cement replacement materials can also be added to concrete. Silica fume can be added in concrete which results in decrease in porosity, permeability and bleeding. It is one of the most popular pozzolans because their oxides (SiO_2) react and utilize calcium hydroxides that are hydration products of ordinary Portland cement. Lower release of heat, development of greater strength, consumption of lime and smaller pore size distribution are the major results of pozzolanic reactions [6].

2.8 Silica Fume

Ferrosilicon and silicon industry produce silica fume (SF) as a byproduct. At 2000°C , SiO_2 vapors are formed by reduction of quartz to silicon. These vapors in the zone of low temperature oxidize and condense to form little non-crystalline silica particles. The percentage of SiO_2 in silica depends upon the alloy used [58]. Normally it is found in grey or premium white color [59]. SF particles are very fine, spherical and amorphous contains small amounts of alkali oxides.

2.8.1 Advantages of using silica fume

SF is commonly utilized for making high strength concrete. Below are the important advantages of SF.

- By using SF, we can get higher early compressive strength
- Higher modulus, tensile and flexural strength
- By using SF, toughness and bond strength can be increased
- Durability is enhanced

- Abrasion resistance is increased
- Increased retardance to chemical attack.

2.8.2 Reaction mechanism of silica fume

SF has finer amorphous silicon dioxide particles that make SF a very reactive pozzolanic material. Basically, SF has three major roles in concrete: (i) Provide dense matrix and reduce the pore size (ii) SF reacts with free lime and produce CSH gel and (iii) refinement of cement paste-aggregate interfacial. SF particles size is very small and they provide the site for nucleation and also react with free lime to form gel. It also changes the orientation of CH crystals and also reduces the transition phase. Hence, improved mechanical properties and enhanced durability can be achieved by using SF [59].

2.8.3 Effect of silica fume on the hardened properties of concrete

2.8.3.1 Compressive strength

Compressive strength is considered as an important mechanical property of concrete. Compressive strength is directly proportional to concrete other positive qualities. By evaluation of concrete compressive strength, a common assessment about the quality of concrete can be achieved.

Mazloom [6] observed the compressive strength of high-strength concrete up to 400 days by varying percentage of silica fume. Silica fume concrete has 21% greater strength than control concrete at the age of 28 days. There is not a significant change in strength after 90 days and then compressive strength again increases after one year. Sobolev (2004) [60] observed the compressive strength of high performance concretes. Silica fume was 5% to 15% of cement and results indicate that concrete having silica fume gave maximum compressive strength at 15% content of silica fume. Wong and Razak (2005) [61] also observed that silica fume enhanced the strength after 7 days. They also concluded that changing w/c from 0.3 to 0.27 did not considerably change the strength.

Köksal et al. (2008) [62] studied on compressive strength using silica and steel fibers. They concluded that by increasing quantity of silica fume without using fibers, compressive strength of concrete increases. Concrete having 15% silica showed 85% increase in strength as compared to mixture having no silica fume.

Hooton (1993) studied the compressive strength by replacement of silica fume 5% to 20% for 5 years. Concrete having silica fume has higher strength at 7 to 91 days and after that the increase in strength was very low as compared to controlled concrete.

Almusallam et al. (2004) [63] concluded that the strength of concrete increases with the increase of silica fume and with the age. The concrete having 15% silica has higher strength.

Babu and Babu (2003) [64] studied the strength behavior of concrete having silica fume, light weight aggregates and expanded polystyrene. They used 3, 5 and 9% of silica and results indicate that by increasing silica fume percentage the strength gains rate increases.

2.8.3.2 Splitting tensile strength

Tensile strength is an essential and basic property which affect the size and extent of cracking in structures. Due to the brittle nature of concrete, its tensile capacity is very less. Also due to very lower thermal expansion coefficient, concrete structures are highly liable to tensile failure. Concrete tensile capacity can be determined with the help of splitting tensile test.

Bhanja and Sengupta (2005) [65] studied the effect of silica on high performance concrete. Results indicate that increase in tensile strength was insignificant when percentage of silica is greater than 15%.

Almusallam et al. (2004) [63] by their experimental work concluded that tensile strength increases with the age of concrete having 15% silica fume.

Köksal et al. (2008) [62] in their research work concluded that there is a considerable increase in tensile strength of concrete by increasing contents of silica fume. For 15% silica fume the increase was almost 88% as compared to controlled concrete.

2.8.3.3 Modulus of elasticity

Modulus of elasticity is related to stiffness of material. It depends on the quality and nature of materials used for formation of concrete matrix.

Mazloom et al. (2004) [6] concluded that secant modulus increased by increasing replacement level of silica fume. At 15% replacement, the modulus increases from 28.8 GPa to 38 GPa.

Almusallam et al. (2004) [63] also studied silica fume effect on elastic modulus of mixtures by using different aggregate types. Results showed that higher the level of silica than higher is the elastic modulus of concrete.

Guneyisi et al. (2004) [66] observed rubberized concrete elastic modulus. They determined that by lowering w/cm, the elastic modulus value increases and the mix having silica fume has slightly greater value of elasticity modulus. The replacement level of silica was 5%-20% and

results express there is not a substantial effect on elastic modulus by increasing the replacement level.

2.9 Effect of Elevated Temperatures on HSC

2.9.1 Introduction

Concrete can be vulnerable to elevated temperatures near to the furnaces or during fire [11]. Although concrete is non-combustible material but fire effect its physical, chemical as well as mechanical properties [67]. Load carrying capacity of buildings are effected after fire exposure [8]. According to Hager (2013) [68] fire effect the concrete strength due to physical and chemical changes occurs in aggregates when temperature rises up to 600°C. Aggregate types and properties play important role in concrete exposed to fire [12].

High strength concrete is susceptible to spalling because of lower permeability and lower thermal conductivity. High temperature results in increased pore pressure due to slow rate of moisture escape. The spalling usually occurs at initial stages of fire because of water expulsion and the thermal expansion effect in concrete mixes. As a result, load carrying capacity of concrete during fire exposures reduces.

2.9.2 Microstructural and Chemical properties

Fire has substantial effects on chemical composition of concrete. Significant removal of chemically bounded water from CSH gel occur above about 110°C [12]. Shrinkage of concrete occur due to disengagement of Calcium hydroxide $[Ca(OH)_2]$ around 530°C [40]. Surface cracking of concrete and spalling occurs at elevated temperatures [69]. According to Hertz, the CSH gel decayed around 600°C and concrete is generally collapse around 800°C [8]. Therefore, concrete strength reduces at elevated temperature due to chemical and microstructural changes.

Gupta et al in their research also done scanning electron microscopy (SEM) on concrete mixtures having recycled coarse aggregate vulnerable to high temperature [69]. They observed the micro cracks in the samples after subjected to elevated temperatures because of water loss and increased in pore size. As a result, higher temperature reduces the strength of concrete and causes a higher strain.

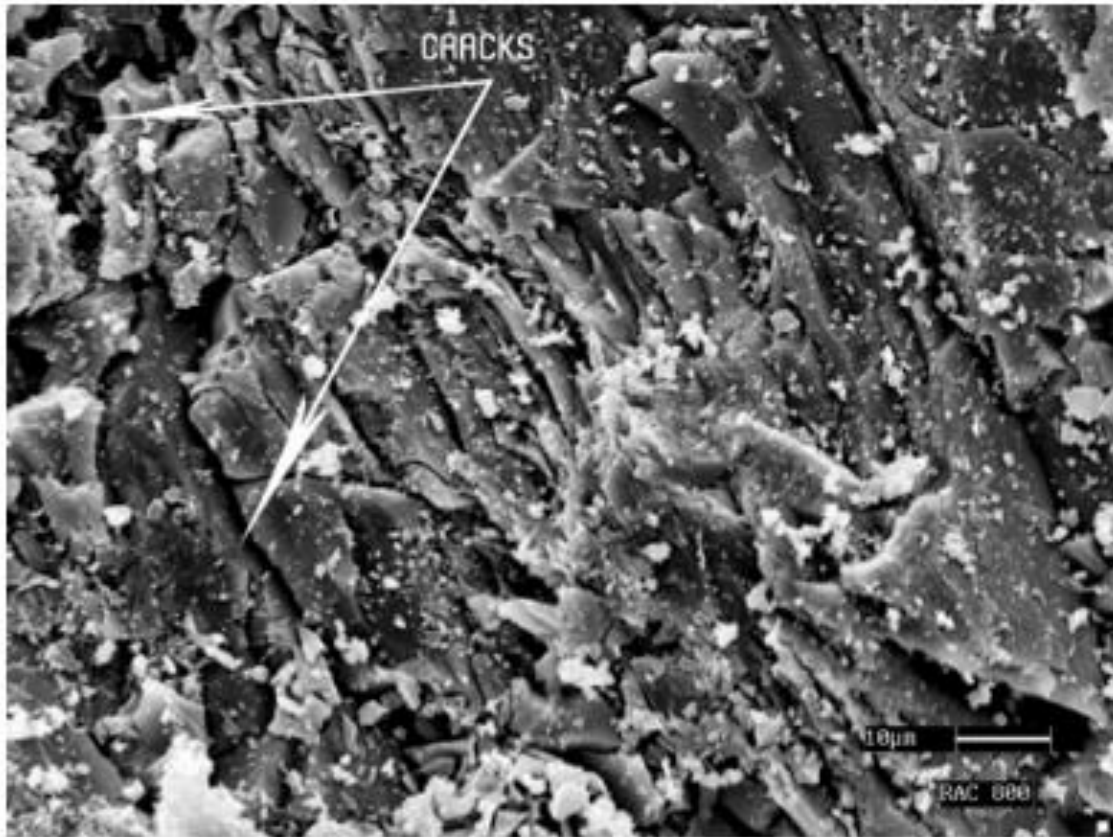


Figure 8 : SEM of concrete sample after exposure to 800°C [69].

2.9.3 Physical properties

The initial assessment of fire damaged concrete usually carried through visual inspection like color change, cracking and spalling [69]. These changes are more evident and permanent when temperature exceeds from 500°C [11].

2.9.3.1 Color, cracking pattern and spalling

Arioz (2007) in his study presented the surface cracking of samples exposed to high temperatures up to 1200°C. Concrete started to show some crack at 600°C and the cracks became obvious at 800°C and comprehensively enhanced at 1000°C [12]. Spalling can be described as explosive breaking of samples into pieces without prior notice. Spalling of samples was noticed after temperature of 1200°C and the samples fully decayed [12].

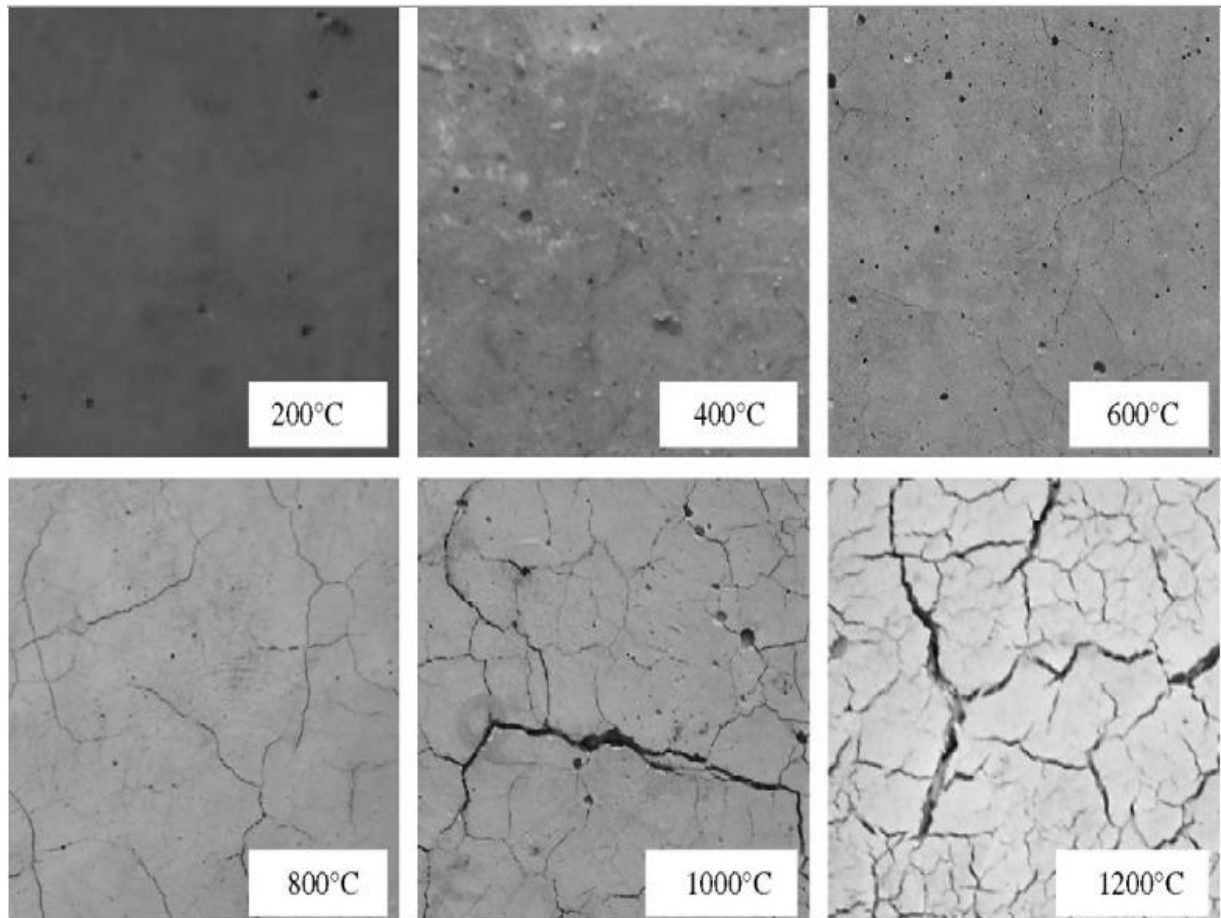


Figure 9 : Surface cracking of concrete samples after exposure to high temperatures [12].

Sofren and Takashi [18] in their study at residual properties of concrete observed explosive spalling of 25% of sample at 370°C.

Khaliq and Waheed [64] in their research on spalling and mechanical response of high strength concrete concluded that the sample having w/cm of 0.3, spall at temperature near 400°C and samples having w/cm of 0.32, spall at temperature near 600°C.

Phan and Carino [71] in their research work reported the spalling of some concrete samples at 450°C and 600°C for stressed and unstressed test conditions for different w/c. Explosive spalling of cylindrical samples occur by the separation of 20mm thick concrete shell. Spalling tendency was lower for stressed test condition as compared to unstressed and residual test conditions and spalling tendency was higher for lower w/cm.

Huzeyfa and Nilufer [72] in their work reported the spalling of concrete above 500°C. Color of samples was changed to red at 300°C, while gray color was observed at 600°C on external surface of the samples and at 900°C, the color was changed to whitish gray.

2.9.3.2 Weight loss

At elevated temperatures loss in weight occurs due to loss of water, transformation in the phase of aggregate and separation of cement [73]. Arioz (2007) [12] in his study observed that the weight loss were 5% and 45% after heating the concrete samples to 200°C and 1200°C, respectively. The weight loss can be due to the alterations in the mechanical properties. Topcu et al (2002) [74] stated that the expulsion of water from C-S-H gel cause reduction in the cement paste bond while water-cement ratio and aggregate type has no significant effect on the weight loss.

Khaliq and Taimur [41] worked on physical and mechanical behavior of recycled aggregates high strength concrete at high temperatures and also compared unstressed and residual test conditions. They concluded that weight loss has no clear pattern and for both conditions, the weight loss was between 13% till 600°C and almost 20% at 800°C.

Khaliq and Waheed [70] in their work on high strength concrete concluded that there were variations in rate of mass loss and mass loss was only between 3%-10% up to 600°C and 22% at 800°C.

Huzeyfa and Nilufer [72] in their work reported that the average mass loss of samples exposed to 300°C, 600°C and 900°C were 5.2%, 9.8% and 12.9%, respectively.

2.9.4 Mechanical properties

2.9.4.1 Compressive strength

The compressive strength of concrete exposed to elevated temperature is a considerable attention in fire resistant design. According to Yuzer [75], strength loss can be due to the thermal incompatibility in the concrete components. Additives can enhance the properties of concrete subjected to high temperatures [76].

Rate of heating and heating temperature also affect concrete properties subjected to elevated temperature. Higher vapor pressure develops due to rapid heating rate and results in cracks in concrete. Compressive strength of concrete starts to reduce when concrete heated at 200°C and above that temperature [77].

The decrease in strength after exposure to elevated temperatures was because of dehydration of hydrates of ettringite, CSH gel and the expulsion of capillary pore water [78,79]. Considerable decrease in strength has been reported above 800°C. The higher decrement in strength can be because of de-hydroxylation of calcium hydroxide [79]. The micro-cracks formation in the samples caused the decrement in strength because of transitions in the cement aggregates bond and changes in the interfacial transition zone [80]. As reported by Phan (2000), the explosive spalling of concrete at elevated temperature is because of the internal pore pressure development and thermal stresses which further reduces the strength [39].

Sofren and Takashi [18] in their study concluded that strength reduces to 20% and 36% at 200°C and 400°C respectively as compared to room temperature.

Khaliq and Waheed [70] in their work concluded that unstressed compressive strength of high strength concrete samples were 67%, 67.5%, 53% and 37% at 100, 200, 400 and 600°C respectively as compared to room temperature.

Khaliq and Taimur [41] in their work on mechanical and physical behavior of recycled aggregates high strength concrete at high temperatures, compared unstressed and residual test conditions. Results indicate that at 100°C, the loss in compressive strength was 12% for residual test condition and 22% for unstressed test condition. At 800°C, the compressive strength was 7% for unstressed test condition and 5% for residual test condition.

Behnood and Ziari (2008) [76] concluded that silica fume increased the strength because silica fume react with calcium hydroxide and formed calcium silicate hydrate (CSH) gel. Silica fume also act as a filler and reduced the porosity. Reductions in strength occurred in the temperature range of 300-600°C, which were 68.8%, 70.9% and 73.2% in concrete containing 0%, 6% and 10% of silica fume, respectively. At elevated temperature, the cement paste and aggregates bonding weakened due to cement paste contraction and aggregates expansion and consequently significant reduction in strength occur.

Phan and Carino [71] in their research worked on three conditions of heating. For temperatures of 100 and 200°C, the residual property test method showed lowest strength loss. For 450°C, the strength loss was highest for the residual property test condition.

Huzeyfa and Nilufer [72] in their work reported that strength reduces with the increase in temperature and also decreases more in smaller size samples. They also concluded that samples having air entrainment agent and fibers shows greater residual strength as compared to controlled specimens.

2.9.4.2 Splitting tensile strength at elevated temperature

Tanyildizi and Coskun (2008) [81] studied silica fume behavior at high temperature by using 10%, 20% and 30% silica fume. Results showed that silica fume addition helped to better retain the tensile strength of concrete.

Sofren and Takashi [18] in their research work concluded that residual tensile strength reduces to 16% and 30% at 200°C and 400°C, respectively, as compared to room temperature tensile strength.

Khaliq and Waheed [70] in their work on high strength concrete concluded that unstressed splitting tensile strength of high strength concrete samples were 72%, 73%, 55% and 24% at 100, 200, 400 and 600°C, respectively, as compared to room temperature.

Khaliq and Taimur [41] in their work compared unstressed and residual test conditions. They concluded that there are no considerable differences in tensile strength response under unstressed and residual test methods. At 800°C, the tensile strength was 16% as compared to room temperature tensile strength.

2.9.4.3 Elastic modulus at elevated temperature

Sofren and Takashi [18] in their research work concluded that elastic modulus of high strength concrete subject to high temperature reduces to 25% and 57% at 200°C and 400°C, respectively, as compared to room temperature.

Khaliq and Waheed [70] concluded that elastic modulus of high strength concrete samples reduces as the temperature is increased and it reduced to 40% at 600°C.

Khaliq and Taimur [41] in their work compared unstressed and residual test conditions. They concluded that loss in elastic modulus was more under unstressed test condition as compared to residual test condition. They also concluded that in unstressed test condition, the loss in

elastic modulus was 26%, 67.7% and 87.3% at 400, 600 and 800°C, respectively, as compared to room temperature.

Phan and Carino [71] in their research work on high strength concrete at high temperature concluded that elastic modulus reduces linearly with the increment of temperature.

2.10 Effect of GNPs on Cementitious composites and Concrete

With the remarkable features of strong adaptability, mature production phase and abundant resources, concrete is widely utilized in the world for construction works. With proper combination of supplementary cementitious materials, cement and low water-to-cement (w/c) ratio, different types of concrete are produced for various purposes. For instance, steel fiber reinforcement is used to enhance tensile strength and to bridge the micro cracks but it increases the cost, self-weight and is also ineffective in delaying micro cracks due to large spacing and less interlocking [1–3]. However, with the development of modern infrastructures, single function of traditional concrete technology is not enough for required multifunctional properties in construction. There is more requirement for advanced materials with enhanced properties to fulfill modern requirements or to replace current materials. In recent years, micro and nano materials have achieved remarkable consideration in the construction material field. Vision, intentions and capability to manage the world of material has changed because of nanotechnology, and it will continue to change [23,24]. The field of construction and materials will surely be affected by these developments. Many research studies describe the capacity of different types of carbon nano materials in the enhancement of cementitious materials which includes carbon nanotubes, carbon nano fibers and carbon black [25,29]. Carbon nano fibers (CNF), carbon nano tube (CNT) and graphite nano platelets (GNPs) have been used to provide nano scale reinforcement for the improvement of thermal properties and to enhance cracking resistance of these materials [26,27,30].

These nano scale materials have high surface area which promotes the growth of hydration products like CSH gel on their surface and makes them efficient in suppressing initiation and spreading of micro cracks and hence improve the mechanical as well as thermal properties [82,83].

2.10.1 GNPs effect on mechanical and thermal properties

The research on GNPs is in its beginning phase [27,84]. GNPs made up of small sacks of graphene having thickness of usually 0.35-100 nm and work as different types of functional filler for cementitious composite [85]. Graphene comprises of hexagonal plane made up of

single carbon-carbon layer and is named as “sub structure unit”. Therefore, the structure of GNPs consists of a net like structure made up of multilayer carbon-carbon hexagonal plane and graphene is a special case of GNPs that contains only one layer of carbon atoms. As a result, the properties of GNPs are regarded as close to graphene [86]. Generally, these GNPs are prepared by intercalation method and then further exfoliated by thermal treatment [33,34]. Similar to CNTs, GNPs possess excellent thermal and electrical conductivities along with improved mechanical properties at ambient conditions[35,36].

Compared with CNTs (8\$/gram), GNPs (2\$/kg) have lower unit cost and also free from entanglement problem [22]. GNPs have favorable surface that increases interfacial bonding to cement paste. Blocking and diversion of cracks at micro and nano level due to plates feature and delaying of cracks initiation due to bridging effect makes GNPs a material having excellent mechanical and thermal properties [22,24,37,38,52]. GNPs can be an excellent alternative for the expensive carbon nano tubes.

In different studies, fibers and CNTs are used to overcome the adverse effects of fire [25,87]. But as already mentioned, these are not very cost effective and furthermore fibers are not effective in resisting the cracks at micro level due to large spacing between fibers [52].

GNPs got more attention in different fields. Different studies have shown the hardness of graphite sheet of single layer to be more than 100 GPa which is harder than diamond [31]. As a result, the hardness of cementitious composites improved by adding GNPs into these composites [32,88].

Huang [27] obtained an increase of 80% in flexural strength and 20% in compressive strength by using GNPs in cementitious materials and results indicate that for mortar optimum value of GNP was 0.05% and for paste 0.5% by using surfactant without sonication.

Mehdi Karevan and Kyria Kalaitzidou [24] in their study on reinforced polymer composites used up to 15% of GNPs and concluded that composites have higher tensile strength at 1% of GNPs.

Weina Meng and Kamal H. Khayat [52] studied the effect of GNP (used up to 0.3% of GNPs) on ultrahigh strength concrete and concluded that GNPs increases the compressive strength, tensile strength (40%) and energy absorption (150%) as compared to controlled samples due to bridging and filler effect of nano material.

Swetha Chandrasekaran, Christian Seidel, Karl Schulte (2013) [23] used GNPs in epoxy nano composites and studied their mechanical, electrical and thermal properties. They used up to 2% weight of concrete. They concluded that at 1% weight, conductivity was 3 orders higher in magnitude than controlled samples. Thermal conductivity was increased by 14% using GNPs.

Xia cui et al 2016 [43] used GNP as multi-functional fillers to form cementitious composites. They used 0%, 1% and 5% by volume of GNPs in cementitious composites. They concluded that the GNPs addition can effectively enhance the cementitious composites properties like thermal conductivity raised by 75%.

Raza et al. concluded that GNP/silicone composite containing 20% wt of GNPs had a thermal conductivity of 1.909 W/(m K) which is an 11-fold greater than pure silicone (0.175 W/m K) [84].

Dhruv Bansal et al. 2012 [49] studied on nano graphite-reinforced carbon/carbon composites and concluded that GNPs increases the strength and reduces porosity. They used 0.5%, 1.5%, 3% and 5% wt. of GNP in this study. Best results were obtained at 1.5% wt. of GNP.

Asma Yasmin and Isaac M. Daniel [35] also studied on GNPs/epoxy composites and results showed that GNPs increases the mechanical properties. Composites having 2.5% of GNPs showed higher elastic modulus and tensile strength than the composites have 5% of GNPs.

Jing Liet al 2007 [22] studied on GNPs in epoxy composites. They used up to 2% wt. of GNPs and concluded that 0.3% wt. of GNPs gave optimum values of mechanical properties.

Zhong [36] in review paper on polymer nano composite conclude that GNPs perform better than other carbon based nano composites.

Peyvandi et al [38] used modified GNPs into the concrete pipes in aggressive sanitary sewer environment to enhance durability characteristics and conclude that GNPs perform better.

Some researchers have been done on material properties of these graphite nano/micro platelets (GNMPs) in concrete and epoxy mixtures at ambient temperatures. However, there is no reliable data available on elevated temperature properties of these nano-reinforced high strength concrete. For predicting the elevated temperature properties, a well-founded experimental data and analytical design has been established. This study provides mechanical, durability, physical and microstructural properties of high strength concrete modified with various proportion of GNMPs up to the target temperature of 800°C.

3 Experimental Program

3.1 General

This chapter discourses the methodology and procedures adopted to achieve research goals. The detailed process from preparation of specimen to testing techniques executed to achieve the results has been explained.

Mechanical, material, and physical properties of concrete are required for studying and assessing the performance of nano-modified mixes at high temperatures. Compressive strength, tensile strength, stress-strain response, elastic modulus and mass loss are important material properties. There is sufficient data available in literature on material properties of high strength concrete but no authentic data is available on elevated temperature properties of mixtures modified with GNMPs. Availability of high temperature material properties of nano/micro-modified mixes is critical for assessing the strength degradation with rise in temperature of structures made with these concrete types.

In order to establish the effect of fire on material properties of HSC modified with GNMPs, mechanical and material property tests at high temperature were carried on reference HSC mix and GNMPs modified concrete mixes which include mechanical strength testing like compressive and tensile strength tests, stress strain behavior, elastic modulus, micro structural properties, ultrasonic pulse velocity test and mass loss. All the mechanical and material properties thus evaluated were presented in form of graphs, and generated data was compared with control mixes as well. The collected data was used to formulate simplified mathematical models for various material properties of these modified mixtures as a function of temperature in range of 23-800°C. Experimental design detail, standards, test setup and procedures of testing are described in this chapter.

3.2 Materials

Ordinary Portland cement (OPC) Type-I in conformity with ASTM C150 was used in the preparation of investigated concrete formulations [89]. Properties of OPC are presented in Table 2. The summarized oxide composition in Table 2 is experimentally attained via X-Ray fluorescence (XRF) technique.

Table 2. Physical and chemical properties of concrete.

Chemical Configuration (Oxides)	Content (%)	Physical property	Content
CaO	65.83	Insoluble residue (% mass)	0.46
SiO ₂	18.81	Specific gravity (g/cm ³)	3.15
Al ₂ O ₃	6.96	Specific surface area (cm ² /g)	8400
Fe ₂ O ₃	3.45	Particle size (d ₅₀) (um)	16.59
MgO	1.95	Loss on ignition (% mass)	1.76
SO ₃	1.31		
Na ₂ O + K ₂ O	1.2		

Natural sand as fine aggregate was used. The natural crushed aggregates of maximum size of 12.5 mm were used as coarse aggregates. Table 3 summarizes the properties of fine and coarse aggregates.

Table 3. Physical properties of fine and coarse aggregates

Aggregate type	Coarse aggregate	Fine aggregate
Size (mm)	12.5	-
Specific gravity (g/cm ³)	2.58	2.64
Water absorption (%)	1	1.59
Bulk density (kg/m ³)	1564	1550

Crushing value	21%	-
Fineness modulus	2.76	2.18
Maximum size of aggregate (mm)	12.5	-

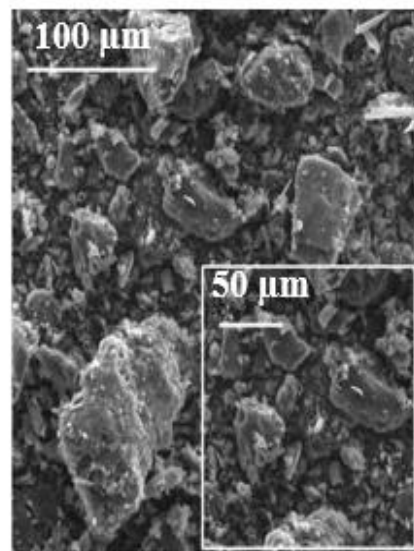
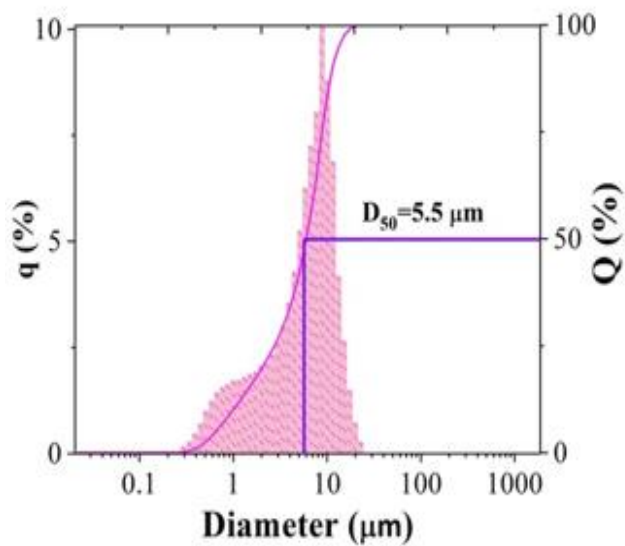
Silica fume was used for improving the properties of concrete and to attain high strength as per ACI 363R-10 [90]. Graphite nano/micro platelets (GNMPs) were used for the modified high strength concrete formulations. Commercially procured GNMPs were subjected to physical and morphological investigation by performing particle size analysis (PSA) and field emission scanning electron microscopy (FESEM), respectively. PSA shown in Figure 10 (a) indicates GNMPs having significant nano and micro-sized particles with their size ranging from 0.29 μm to 22.79 μm with a median size (D_{50}) of 5.5 μm . FESEM results in Figure 10 (b) indicate predominantly irregular shaped particles including platelets. Energy dispersive spectroscopy (EDS) data shown in Figure 11 provides the elemental percentages of graphite. The results shown in Table 4 suggest pure carbon concentration of around 97.69%. Acacia gum/Gum Arabic was used as surfactant for the dispersion of the GNMPs. Elemental composition of gum Arabic is shown in Table 5.

Table 4. Elemental elements of raw graphite

Element	Weight%	Atomic%
C	97.69	98.26
O	2.3	1.74
Si	0.01	0.01
Total	100	100

Table 5. Elemental composition of Gum Arabic

Element	Weight%	Atomic%
C	66.81	73.70
O	31.01	25.69
Na	0.24	0.14
K	0.20	0.07
Ca	0.84	0.28
Mo	0.90	0.12
Total	100	100



a) PSA of Graphite

b) FESEM of Graphite

Figure 10 : Particle size analysis and FESEM of graphite

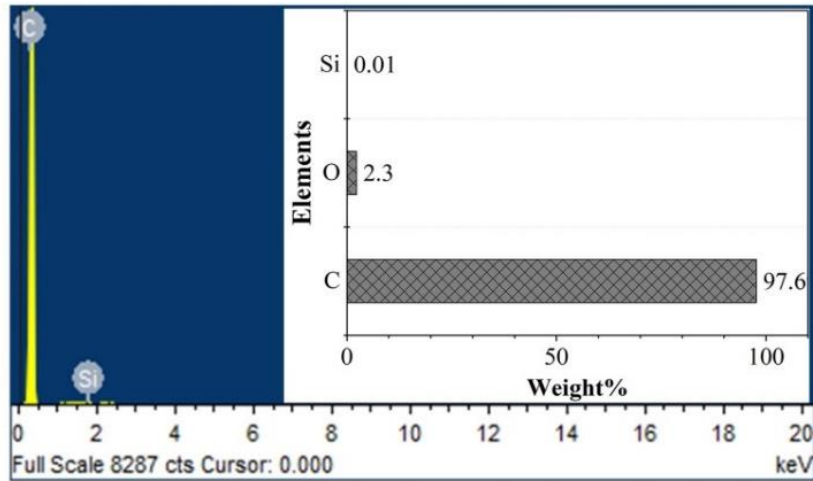


Figure 11 : EDS of Graphite

3.3 Mix proportions and preparation of specimen

A control high strength concrete (HSC) formulation and three modified formulations of high strength concrete containing GNMPs of 0.1% (0.1GNMPs), 0.3% (0.3GNMPs) and 0.5% (0.5GNMPs) were prepared using water to cement ratio of 0.27. Third generation superplasticizer (Sika ViscoCrete-3110) 1% by weight of cement was used to adjust the slump of concrete mixture to 100 mm. Cylindrical specimens (100 mm x 200 mm) were prepared and de-molded after 24 hours of casting. For curing, specimens were placed in controlled conditions as specified in ASTM C192 (23°C ±2°C, 95% humidity) [91]. Development of compressive strength was observed by ASTM C39 [92]. Table 6 shows the mix design detail and the strength progression of analyzed formulations.

Table 6. Detail of mixture proportions and strength progression

Mix	Cement	GNMPs	Silica	Water (w/c=0.27)	Fine Aggregates	Coarse Aggregates
	kg/m ³	kg/m ³	kg/m ³	kg/m ³	kg/m ³	kg/m ³
HSC	713	0	71	192	802	820
0.1GNMPs	713	0.713	71	192	802	820
0.3GNMPs	713	2.14	71	192	802	820
0.5GNMPs	713	3.56	71	192	802	820
Compressive Strength (MPa)						
	HSC	0.1GNMPs	0.3GNMPs	0.5GNMPs		
3 days	19.10	23.21	24.68	23.51		
7 days	31.67	36.20	40.65	39.35		
14 days	37.40	46.41	49.20	48.10		
28 days	47.98	57.95	61.46	59.62		

3.4 Target temperatures for test methods

The target temperatures achieved in this study are 23°C, 100°C, 200°C, 400°C, 600°C and 800°C.

3.5 Test equipment and procedure

The samples of concrete were subjected to elevated temperatures by using an electric furnace (shown in Figure 12) with capability to sustain temperatures up to 1100°C. Electric furnace was assembled with a temperature rate controller and hold time controller.



Figure 12 : Electric Furnace for heating the samples to targeted temperatures

In order to obtain the compressive strength values by ASTM C39 [86], concrete samples were examined using a load-controlled universal testing machine (UTM) having 1000 KN capacity to resist compressive loading (shown in Figure 13). Loading rate of 0.20 MPa/second was applied to record the mechanical response in compression. Modulus of elasticity was obtained as per ASTM C469 procedure [87]. For tensile strength, concrete specimens were tested diametrically by ASTM C496 method [93]. All the exposure temperatures were provided with

holding time of 2 hours and 30 minutes. In order to achieve uniform thermal state a minimum holding time of 2 hours is required as concrete has low thermal conductivity [25,94]. The targeted temperatures in this study were 23°C, 100°C, 200°C, 400°C, 600°C and 800°C. RILEM test procedures were adopted for heating rate and hold times [95,96]. The heating rate for specimens to reach targeted temperature was 5°C/minute. Samples were allowed to cool down slowly to ambient temperature with the door of furnace kept open to avoid thermal shock. Prior to strength tests, Ultrasonic pulse velocity (UPV) and mass loss test were performed before and after the heat exposure.



Figure 13 : Universal testing machine for mechanical testing

3.5.1 Compressive strength test

After achieving the thermal steady state temperature condition, samples were cool down to ambient temperature in air and then shifted to compression testing machine in case of residual test conditions. While in case of rapid cooling/quenching condition, specimens were water sprayed and then cool down to ambient temperature in air before they were tested. ASTM C39 [92] was followed to determine compressive strength, as no testing standards are available in

literature which encompass high-temperature compressive testing. Compressive strength $f_{c,T}$ as a function of temperature were thus evaluated at targeted temperatures.

One specimen was tested at each required temperature. If results were found ambiguous or outliers, additional testing was done to confirm results. To draw a comparison amongst results of different concrete types and testing conditions, relative compressive strengths were calculated using following relationship.

$$\text{Relative Compressive Strength} = \frac{\text{Strength at targeted temperature}}{\text{Ambient temperature strength}} \dots\dots\dots \text{EQ.1}$$

3.5.2 Splitting tensile strength

The heat-treated samples were allowed to cool down to room temperatures in residual test conditions. The samples were loaded diametrically at the loading rate of 0.02MPa per second and the peak load was recorded. The tensile strength ($f_{t,T}$) were calculated in accordance with ASTM C496 [93]. To compare tensile strength of different types of concretes under different test conditions, relative tensile strength was calculated using following relationship.

$$\text{Relative Tensile Strength} = \frac{\text{Strength at target temperature}}{\text{Ambient temperature strength}} \dots\dots\dots \text{EQ.2}$$

3.5.3 Stress-strain curve

Compressive strength tests were undertaken to achieve stress-strain response of concrete cylinders. Data was obtained by failing cylinders under gradually rising loads at precise loading rate of 0.2MPa/second.

3.5.4 Elastic modulus

The elastic modulus of concrete samples was evaluated using the stress-strain curves. Chord modulus of elasticity was calculated using relationship described in ASTM C469 [97].

$$E = \frac{S_2 - S_1}{\epsilon_2 - \epsilon_1} \dots\dots\dots \text{EQ.3}$$

E = Chord modulus of elasticity

S₂ = Stress against 40% of ultimate load

S₁ = Stress against longitudinal strain of 0.00005

ε₁ = Longitudinal strain against S₁=0.00005

ϵ_2 = Longitudinal strain against S_2

3.5.5 Mass loss

To calculate variation in mass of heat-treated concrete samples, they were weighed before and after heat treatment. For residual and quenching conditions, heat treated samples were cool down to ambient temperature before mass loss measurements. The specimens then transferred to sensitive balance (1000th of a kilogram) and weighed to record the change in weight at a particular target temperature. Relative mass loss measured at different temperatures was calculated from the following relationship.

$$\text{Mass loss} = \frac{M_t}{M} \dots \dots \dots \text{EQ.4}$$

M_t = Mass at temperature (T)

M = Mass at ambient temperature

3.5.6 Non-Destructive Testing

The process of inspection, testing and evaluation of materials, systems, elements or sections for disruption or distinction in the features and quality without shattering or demolition, is known as nondestructive testing (NDT). The element would remain unaltered even after the inspection is completed. Physical properties like compressive strength could be determine by using NDT process.

3.5.6.1 Ultrasonic Pulse Velocity Test (UPV)

The quality of concrete is assessed by adopting this method, in which ultrasonic pulse velocity is passed in the concrete and time of travel is measured. Higher velocity depicts the good quality of concrete in terms of homogeneity, density, uniformity and strength. This test was performed according to ASTM C597 [98].

4 Results and discussion

Test results of mechanical properties such as tensile strength, compressive strength, stress-strain response, modulus of elasticity, ultrasonic pulse velocity, micro structural analysis, visual assessment and mass loss under different test condition are analyzed for high strength concrete and nano/micro graphite platelets modified high strength concrete.

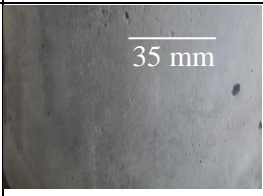
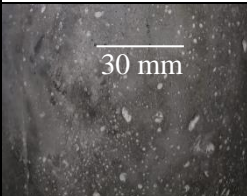

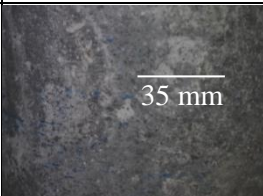
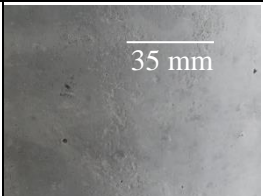



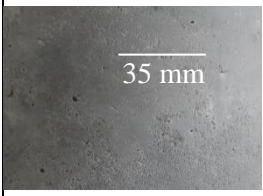
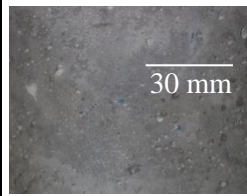


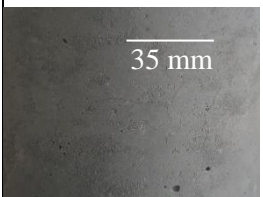
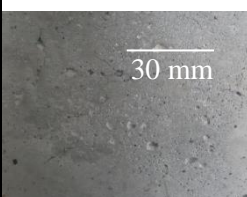
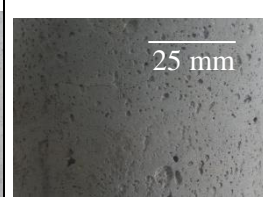

4.1 Visual assessment and spalling of concrete

Visual assessment is the first tool to access the serviceability and condition of a fire damaged structure. Thus, making visual inspection of concrete to be of paramount importance. Visual assessments of heated specimens were performed to examine any changes of color, crazing, or cracking patterns for assessing the serviceability of concrete after being exposed to fire as shown in Figure 14 and 15. The color of a fire damaged concrete sample serves for the comprehensive concept regarding temperature to which it has been exposed. Loss of water, dehydration of paste and microstructure disintegration at high temperature are the major causes of crazing and thermal cracking in concrete [94].

The visual analysis of reference HSC samples revealed no considerable change in color till 400°C. Although, above 600°C, change of color from greyish to light grey color was observed. However, GNMPs concrete showed a peculiar color behavior. 0.1GNMPs concrete showed dark grey color at 23°C. At 400°C, the color was transformed to grey, while it turned to light grey at 600°C. 0.3GNMPs concrete color was greyish black at 23°C. At 400°C, the color transformed to grey and then to light grey after exposure to 600°C. 0.5GNMPs concrete color was light-black in ambient, later turned into greyish black at 200°C and then turned into grey at 600°C.

In all the concrete types, no significant cracking and crazing was observed till 200°C. At 400°C, surface cracks were developed in all the investigated formulations but these cracks were relatively wider in HSC as compared to GNMPs mix. After exposure to 600°C, intensive cracking of surface and crazing was noticed in reference as well as in the GNMPs reinforced concrete formulations. Fire induced explosive spalling was observed in HSC concrete samples when temperature reached around 650°C, while the spalling was observed in 0.5GNMPs high strength concrete after hold time of around 30 minutes, when heated to 800°C. Fire induced

spalling in HSC is mostly attributed to accumulation of thermal stresses, which is due to the lower thermal conductivity [99]. The lack of thermal conductive media in control samples led to the occurrence of concentrated heat pockets. Hence, a pattern of concentrated cracks was observed in HSC samples. High thermal conductivity of modified samples dispersed the thermal stresses, because of which cracks were well scattered and in turn improved the thermal stability of modified samples. 0.3GNMPs formulation showed better thermal endurance and did not spall off on experiencing the temperature of 800°C like the reference and 0.5GNMPs modified formulation. The modified response of 0.3GNMPs mix may be attributed to their homogeneous distribution, adequate quantity and high thermal conductivity [23,24,43,84,100].

Temp	HSC	0.1GNMPs	0.3GNMPs	0.5GNMPs
23°C				
100°C				
200°C				
400°C				

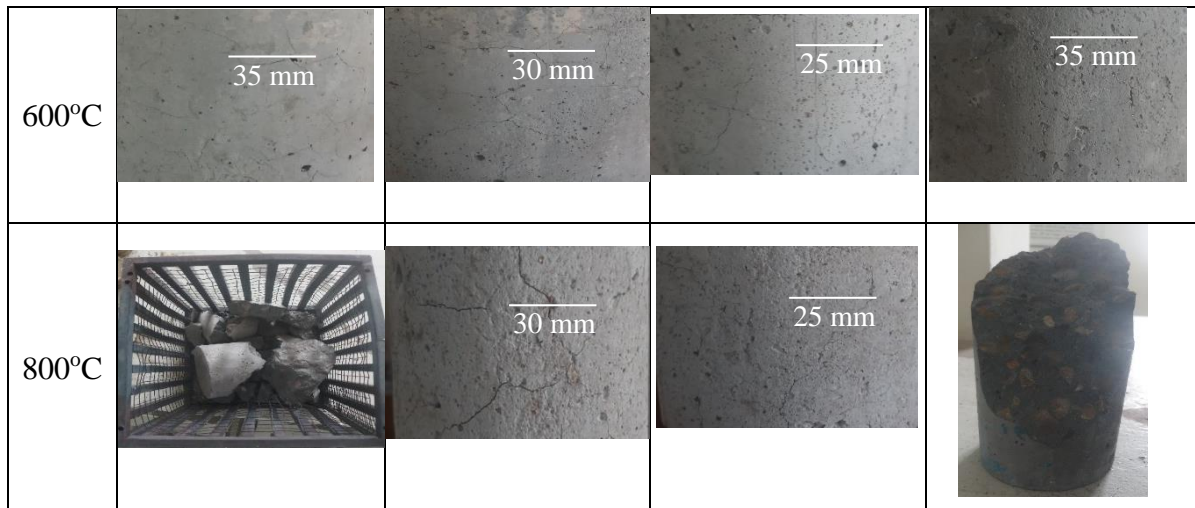
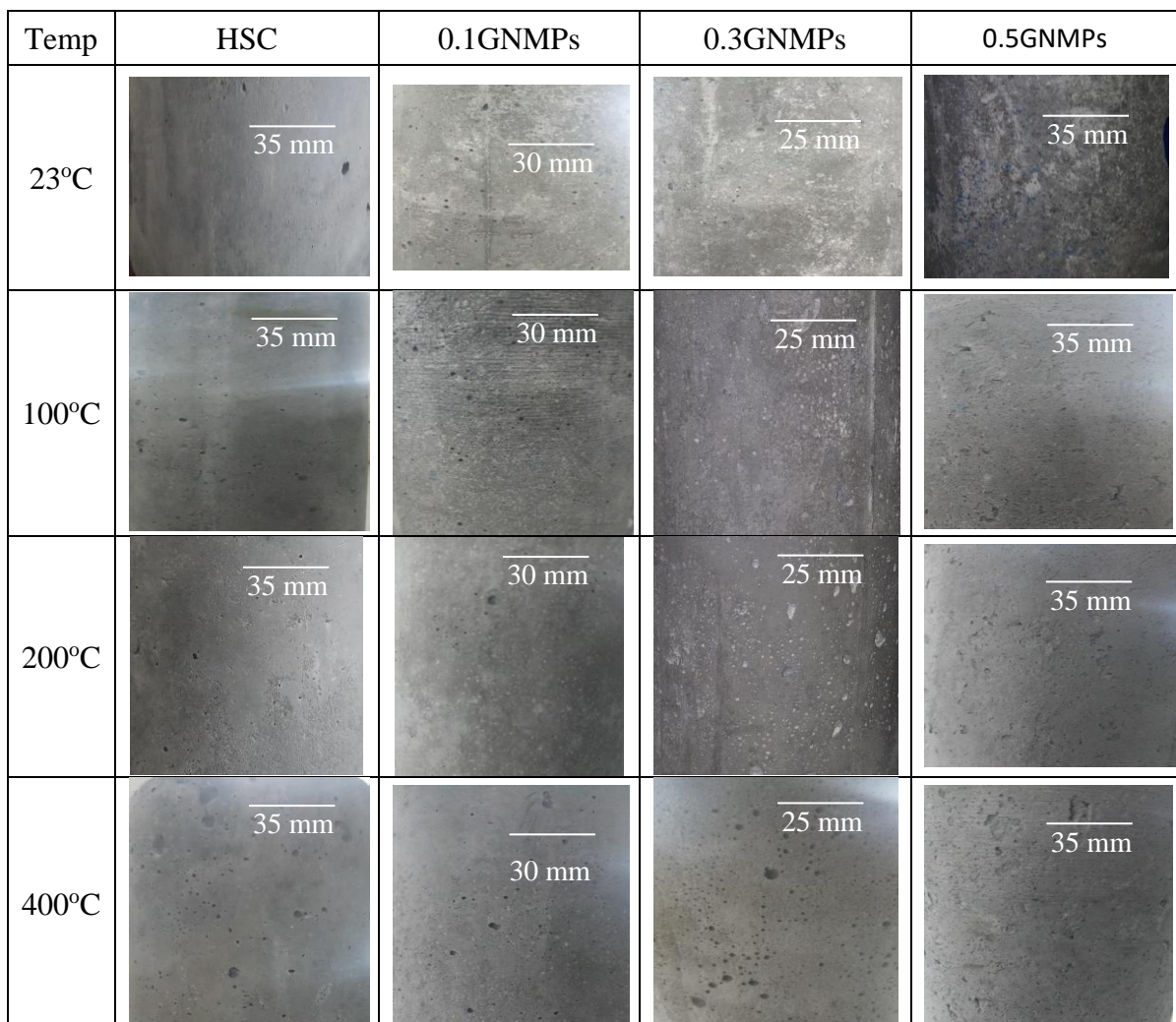


Figure 14 : Color change, cracking and spalling visuals of reference and modified HSC with nano/micro graphite platelets at ambient and elevated temperature conditions (Residual test condition)



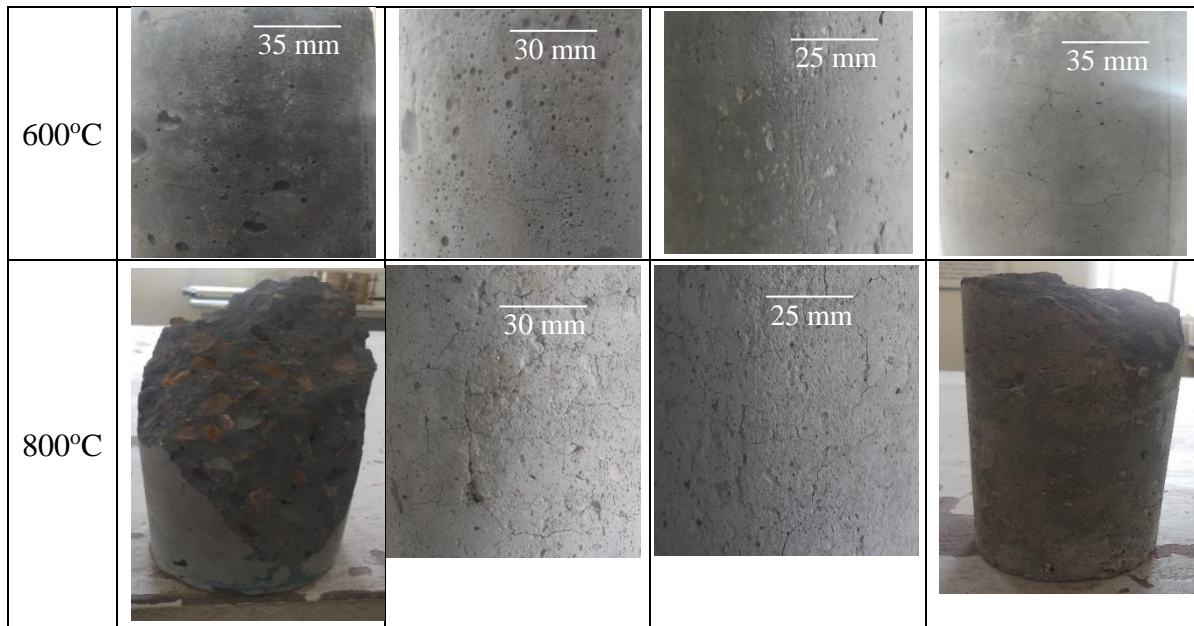


Figure 15 : Color change, cracking and spalling visuals of reference and modified HSC with nano/micro graphite platelets at ambient and elevated temperature conditions (Rapid cooling/Quenching test condition)

4.2 Compressive strength

4.2.1 Compressive strength tests for residual test condition

Figure 16 and 17 shows the values of absolute and relative compressive strengths. It was analyzed that each type of concrete lost its stability when the exposed temperature was increased from 23°C to 800°C. The indicated reduction in compressive strength is due to the change in the physical and chemical composition upon heating. At 600°C, calcium silicate hydrate (CSH) gel decompose which results in significant strength reduction accompanied with loss of stiffness [13]. Upto 600°C, calcium silicate hydrate (C-S-H) gel and calcium hydroxide (CH) decompose that results in significant reduction in strength [71]. Above 600°C, major cause of strength degradation is the instability of aggregates. As de-carbonation of CaCO_3 occurs in the ranges of 600–800°C, resulting in the dissociation of limestone and subsequent loss in strength [41,79].

From figure16, it could be found that compressive strength of modified mixes increased by 20%, 28% and 24% by adding 0.1%, 0.3% and 0.5% GNMPs, respectively, compared with HSC mix at ambient temperature. This increment of the compressive strength could be due to filler effect of these particles, that refines the microstructure and tend to increase the degree of cement hydration as well [32,52]. It was observed from the data of performed tests that concrete

having graphite nano/micro platelets exhibited comparatively lower reduction of the compressive strength throughout heating phase of 100-800°C. Upto 100°C, relative compressive strength loss for all samples follow the same trend. However, the strength loss above 200°C becomes more noticeable. At 100°C, loss in the strength was 10%, 12%, 6% and 9% in HSC, 0.1GNMPs, 0.3GNMPs and 0.5GNMPs, respectively. At 200°C, the loss was 27%, 21%, 13% and 18% respectively. At 400°C, nano/micro reinforcement of graphite showed lower strength loss of 41%, 36% and 49% in comparison to 54% in controlled samples. At 600°C, the loss was 64%, 57% and 70% in comparison to 74% loss in HSC. 0.3GNMPs performed better as compared to HSC and other modified formulations. The strength loss in 0.3GNMPs at 100, 200, 400 and 600°C were 6%, 13%, 36% and 57%, while in HSC the losses were 10%, 26%, 54% and 74%, respectively, as compared to ambient temperature strength. The observed trend of results are very related to past research on HSC by Sofren and Takashi [18] and Khaliq and Taimur [41]. As already mentioned, concentrated heat pockets are developed at elevated temperature and thermal stresses are produced. However, due to higher thermal conductivity [43] and uniform dispersion of GNMPs, these thermal stresses are well scattered and dispersed in the modified matrices.

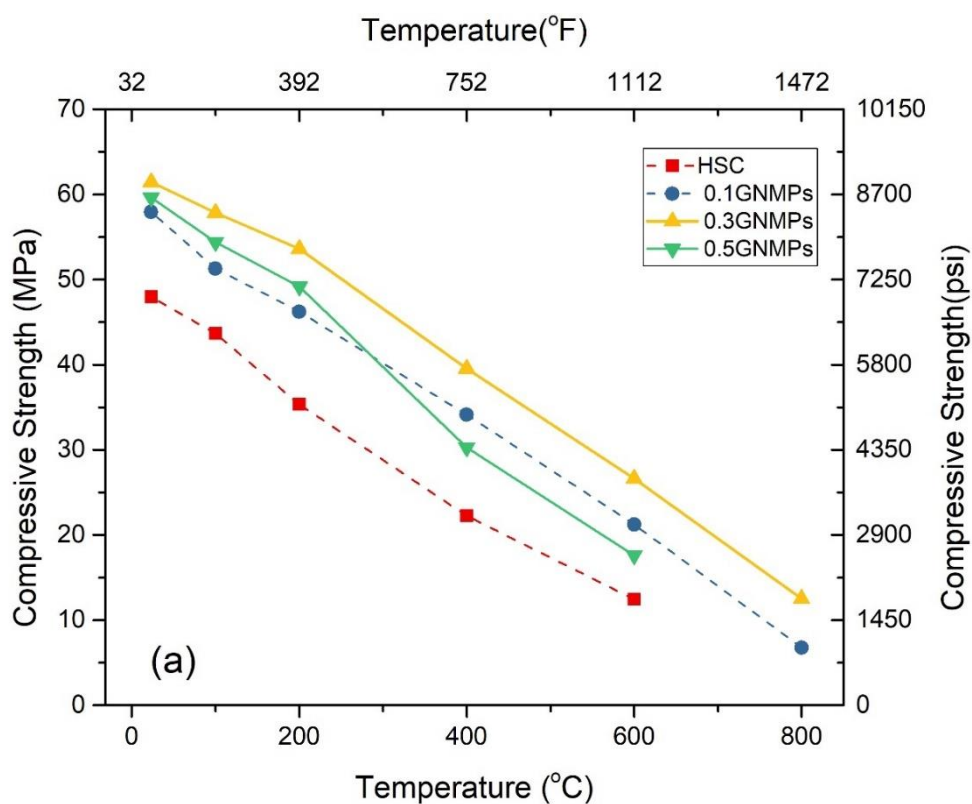


Figure 16 : Variation in absolute compressive strength of HSC and nano/micro graphite platelets modified HSC at ambient and elevated temperatures

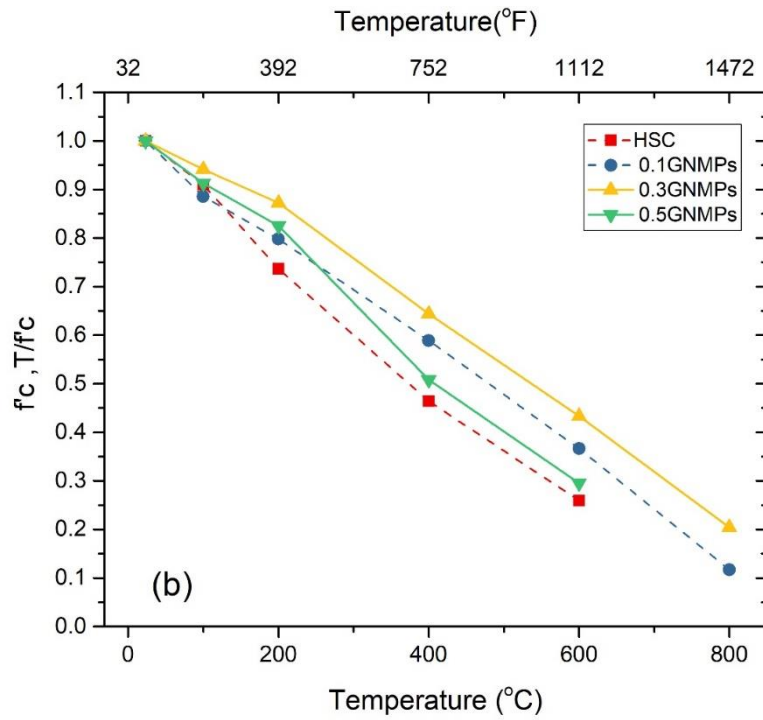


Figure 17 : Variation in relative compressive strength of HSC and nano/micro graphite platelets modified HSC at ambient and elevated temperatures

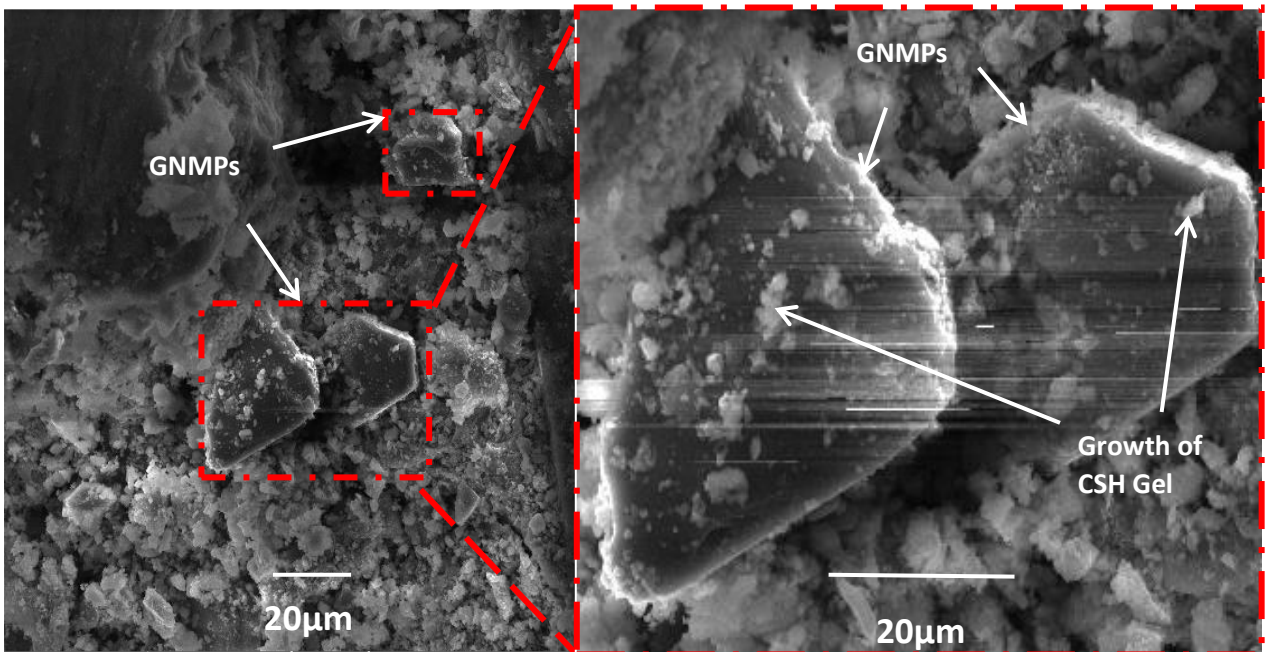


Figure 18 : Micrograph of 0.3GNMPs concrete after being exposed to elevated temperature of 400°C

Moreover, these GNMPs promote the growth of CSH gel on their surface [32] and consequently improve the mechanical properties. Figure 18 showed the microstructure of 0.3GNMPs at 400°C. It can be seen that the GNMPs are well dispersed in the cement phase. Growth of CSH gel can also be seen on the particles of GNMPs in Figure 18, which establishes it being a nucleation site to some extent.

Furthermore, these highly dispersed GNMPs act as heat carrier and ensure its uniform distribution, thereby reduce the quantum of induced thermal stresses. GNMPs possess the “surface effect”, contributing to provide excess interface area, to establish firm binding with the cement grains [37]. The platted configuration of these GNMPs that are well dispersed as in case of 0.1 and 0.3GNMPs, allow to hinder and alter micro and nano level cracks and hence better retain the compressive strength [32,52]. Higher strength loss in 0.5GNMPs as compared to 0.1GNMPs and 0.3GNMPs might be associated with unnecessary flocculation of stiff platelets forming the weak zones [23,35,100].

4.2.2 Compressive strength for rapid cooling/quenching method

It is observed from Figure 19 and 20 that compressive strength of modified mixes increases 20%, 28% and 24% by adding 0.1%, 0.3% and 0.5% GNMPs, respectively, as compared to HSC mix.

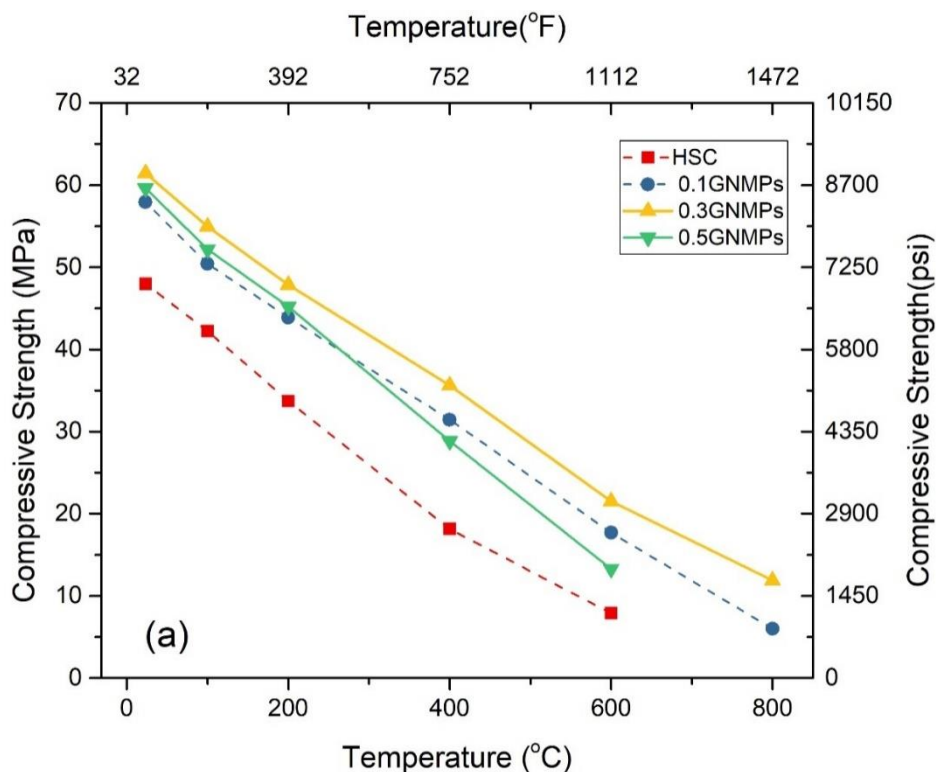


Figure 19 : Variation in relative compressive strength of HSC and nano/micro graphite platelets modified HSC at ambient and elevated temperatures (Rapid cooling/quenching test method)

Due to flaky shape of GNMPs that makes a strong bond between aggregates and other ingredients, gain in compressive strength was observed. At 100°C, loss in strength was 12%, 13%, 11% and 12% in HSC, 0.1GNMPs, 0.3GNMPs and 0.5GNMPs respectively. The loss in compressive strength is because of loss of free water and water present in the C-S-H gel [102]. At 200°C, the loss was 30%, 25%, 23% and 24% respectively.

At 400°C, GNMPs show lower strength loss of 46%, 42% and 52% in comparison to 62% in controlled samples. At 600°C, the loss was 70%, 65% and 78% in comparison to 84% loss in HSC. Loss in strength at 0.5% GNMPs was observed because GNMPs could not disperse uniformly in the concrete matrix due to high concentration. Strength loss in rapid cooling method is greater as compared to residual strength loss. The greater decrement in the strength in fast cooling/quenching method is because of thermal shock in the concrete samples due to rapid cooling [26].

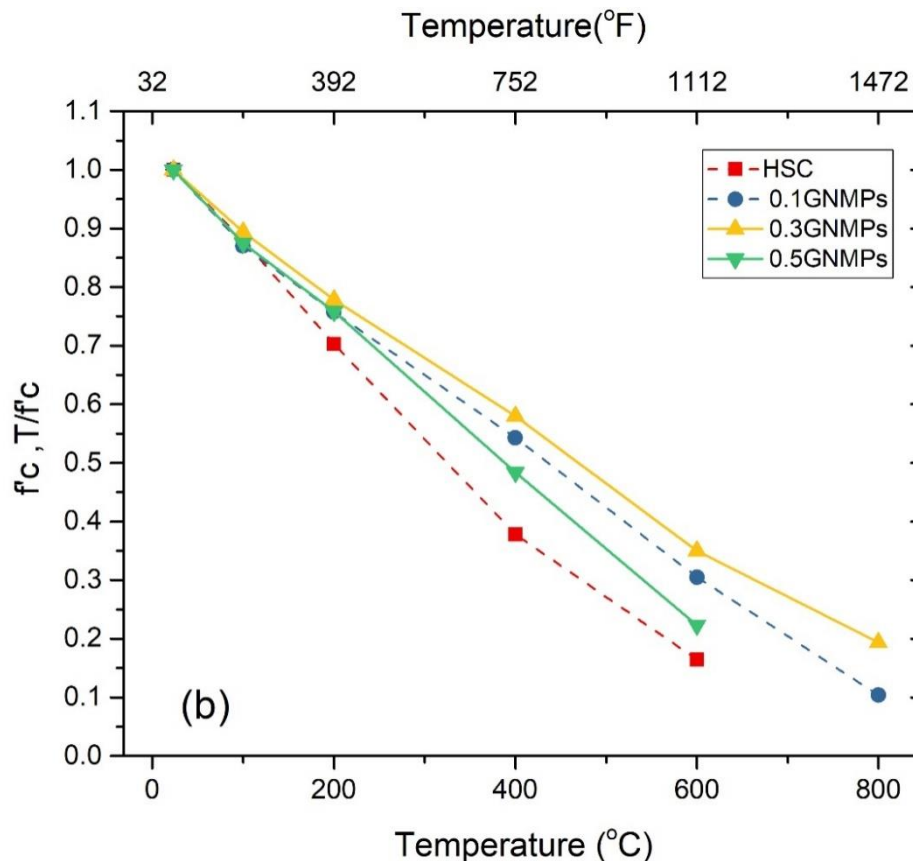


Figure 20: Variation in relative compressive strength of HSC and nano/micro graphite platelets modified HSC at ambient and elevated temperatures (Rapid cooling/quenching test method)

Due to rapid cooling, stresses are generated between outer and inner core of concrete which increases the micro-cracks in the concrete [103]. Initially these cracks do not affect the strength much but as the temperatures goes beyond 200°C, due to generation of tensile stresses on the outer surface the cracks widened up which caused significance loss in strength.

4.3 Tensile strength

ASTM C496 [93] was followed for computation of splitting tensile strength. Because of the inevitable physio-chemical degradation in concrete mix, loss of tensile strength occurred during fire exposure.

4.3.1 Residual tensile strength

It may be observed in Figure 21 that tensile strength of modified mixes improved by 16.3%, 30% and 19% by adding 0.1%, 0.3% and 0.5% GNMPs, respectively, compared to the HSC mix having no GNMPs. There was an increment of tensile strength of mixes along with GNMPs constituents but at 0.5% GNMPs concentration, concrete showed lesser increment in tensile strength that might be attributed to inadequate dispersion of stiff platelets, leading towards agglomerate formations [23,49,100]. Because of the inevitable physic-o-chemical degradation of concrete mix upon heat exposure, loss of tensile strength occurred on subjection to fire.

HSC showed higher strength loss of 28%, 38%, 60% and 84% at 100, 200, 400 and 600°C while the strength loss in 0.3GNMPs were 11%, 23%, 42% and 70%, respectively, at the aforementioned targeted temperature. The reduction in tensile strength of HSC is conforms to prior studies by Suhaendi and khaliq [18,70]. Load carrying area of the concrete mix reduces due to inception and propagation of cracks. Furthermore, because of lower thermal conductivity of concrete, thermal stresses are generated at elevated temperatures which produces the thermal cracks and effect the mechanical properties. GNMPs possesses high thermal conductivity and also due to the bridging effect of GNMPs, the process of initiation and opening up of the cracks can be delayed. Apart from this the mechanical properties of nano mixtures can be increased by GNMPs through crack-arresting effect [32,52]. Thus, GNMPs concrete samples showed better performance at elevated temperature as compared to controlled samples.

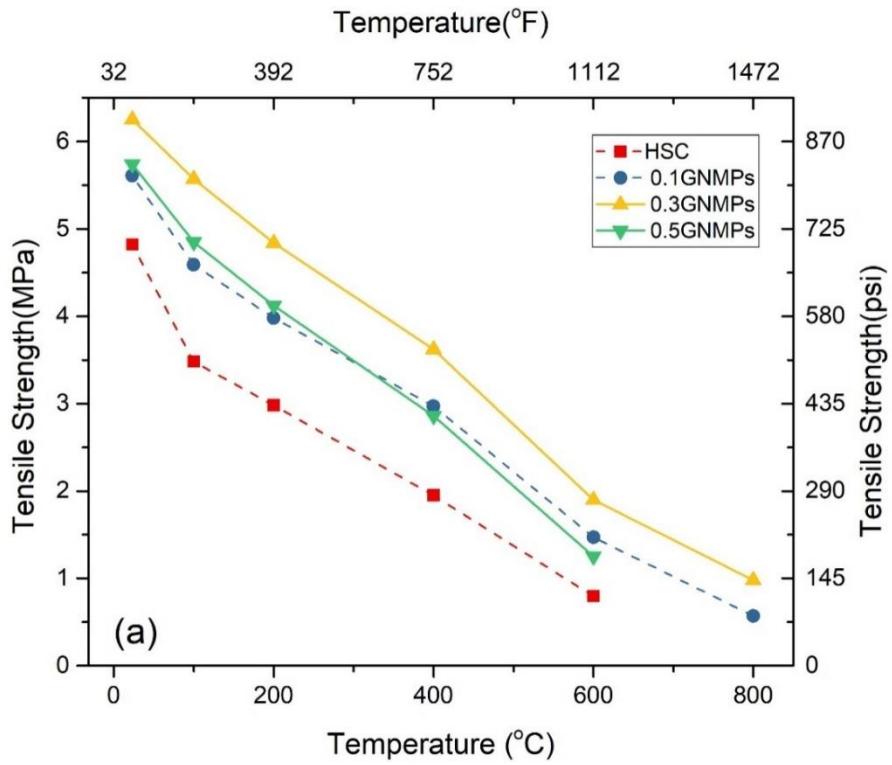


Figure 20: Variation in residual tensile strength of HSC and nano/micro graphite platelets modified HSC at ambient and elevated temperatures

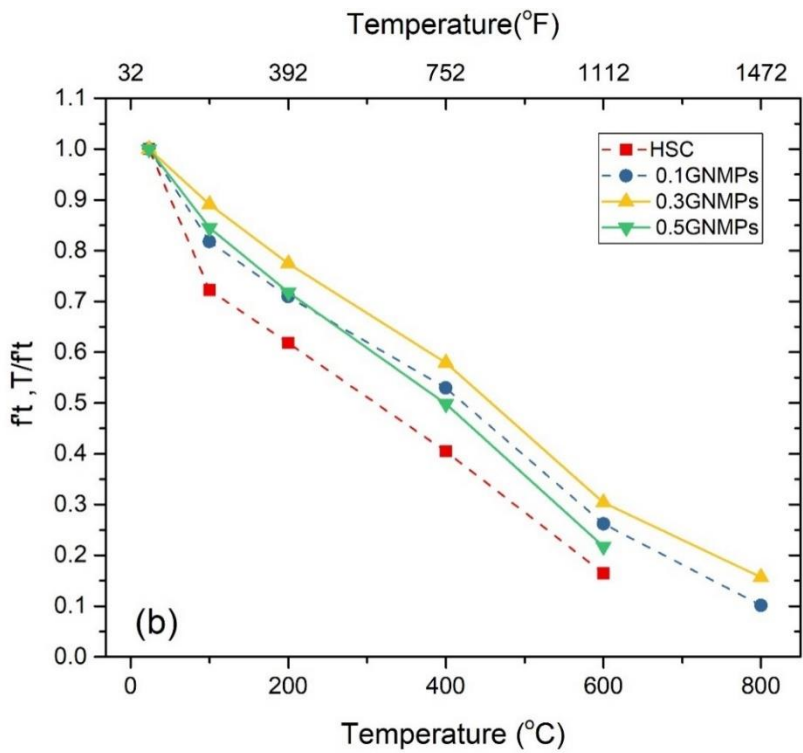


Figure 21: Variation in relative residual tensile strength of HSC and nano/micro graphite platelets modified HSC at ambient and elevated temperatures

4.3.2 Tensile strength for rapid cooling/quenching method

Propagation of micro cracks in concrete highly damages concrete structures. At elevated temperatures tensile strength is more important where spalling phenomenon occurs [70]. As shown in Figure 23 that tensile strength of concrete increased 16.3%, 30% and 19% by adding 0.1%, 0.3% and 0.5% GNMPs, respectively, as compared to HSC mix having no GNMPs.

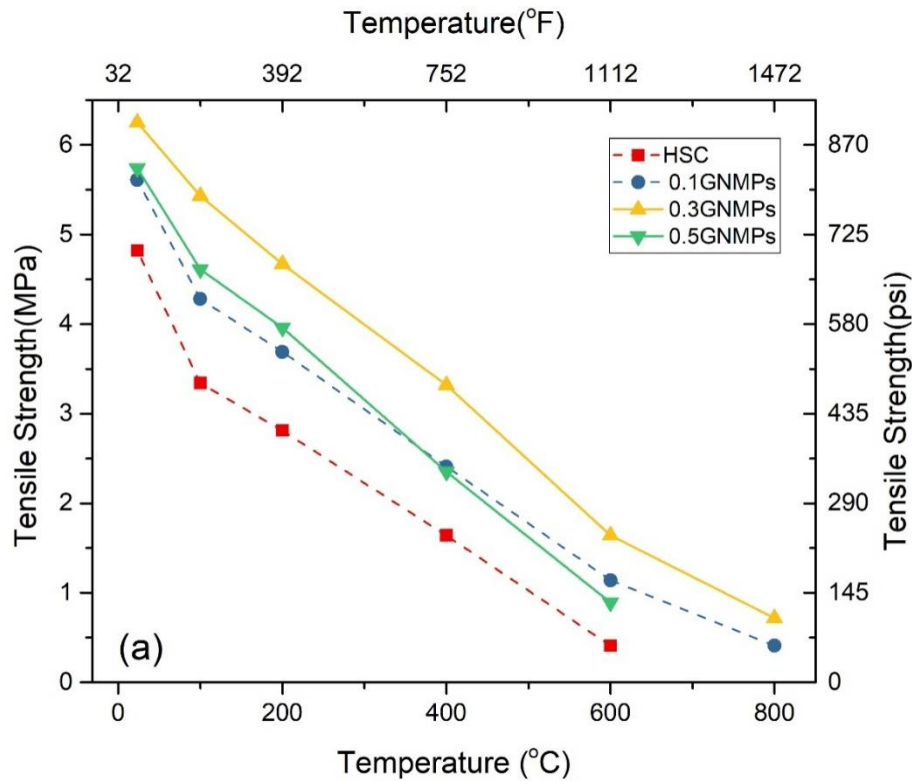


Figure 22 : Variation in absolute tensile strength of HSC and nano/micro graphite platelets modified HSC at ambient and elevated temperatures (Rapid cooling/quenching test method)

At 0.1% and 0.3% of GNMPs tensile strength is increased but at 0.5% concentration of GNMPs, decrease in tensile strength was observed because of non-uniform dispersion of GNMPs due to their high concentration which makes clumps in the mix. At 100°C, loss in tensile strength was 31%, 24%, 14% and 20% in HSC, 0.1GNMPs, 0.3GNMPs and 0.5GNMPs respectively. At 200°C, the loss was 42%, 34%, 26% and 31% respectively. At 400°C, nano/micro reinforcement of graphite shows lower strength loss of 57%, 47% and 60% in comparison to 66% in controlled samples. At 600°C, the loss was 80%, 74% and 85% in comparison to 92% loss in HSC. At 800°C, the loss was 93% and 88% in 0.1GNMPs and 0.3GNMPs. Loss in tensile strength in all the concrete types are also greater in the fast cooling/quenching method as compared to residual method due to high stresses generated in

fast cooling method. According to Yuzer et al [75], during fast cooling, calcium oxide is converted into calcium hydroxide and moves through the pores that results in increase of volume and causes major cracks in concrete.

The flaky shape of GNMPs makes the bonding between the ingredients stronger that helps in resisting the initial cracks in the concrete. Thus, GNMPs concrete showed better performance at elevated temperature in all test conditions as compared to normal HSC.

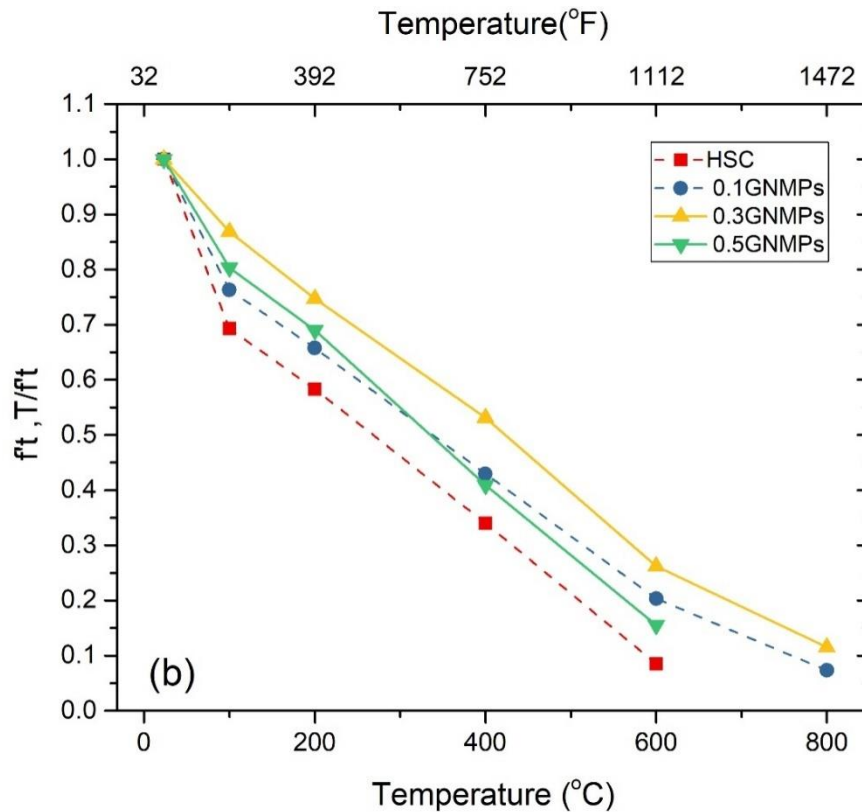


Figure 23 : Variation in relative tensile strength of HSC and nano/micro graphite platelets modified HSC at ambient and elevated temperatures (Rapid cooling/quenching test method)

4.4 Stress-strain response

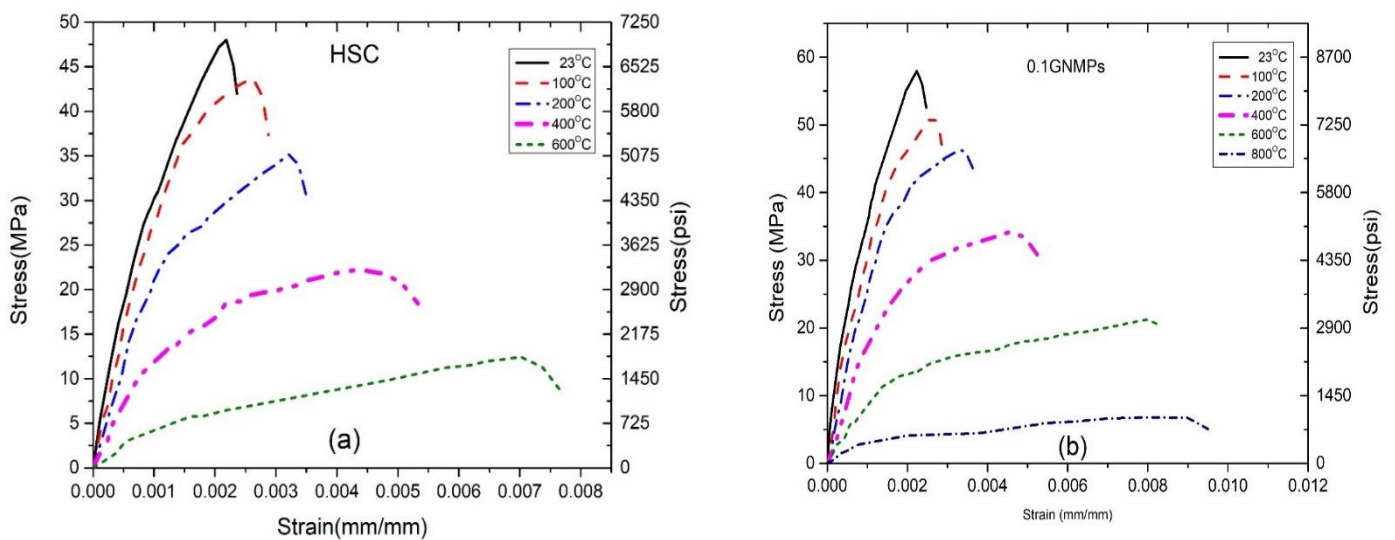
Along with the compression tests, stress-strain response was obtained at each targeted temperature for all high strength concrete types. Load-deformation data was obtained using data acquisition system from UTM.

4.4.1 Residual stress strain response

Figure 25 shows a common trend in stress-strain response that by increase in temperature, the ultimate peak stress decrease and corresponding strains increases for all the analyzed

formulations at each target temperature. This can be due to the alteration in microstructures which involves cracking of mortar, disintegration of bond as a result of paste-aggregate thermal incompatibility, CH decomposition, de-carbonation and CSH gel disintegration [94,104].

The peak strain values for HSC were 22%, 48.2%, 126% and 225% higher after exposure to 100, 200, 400 and 600°C temperatures, as compared to the ambient temperature strain. Similarly, increase in strains with the increase in temperatures were obtained for modified formulations. For 0.3GNMPs the peak strain was 160% and 295% higher after exposure to 400 and 600°C temperatures respectively, as compared to ambient temperature strain. Peak strains of 0.3GNMPs were higher as compared to HSC strain values. The Peak strains values were greater for 0.3GNMPs due to adequate quantity and uniform distribution of GNMPs as shown in the scanning electron micrograph included in figure 18. Expulsion of water at high temperature causes the dehydration of matrix and subsequent development of cracking [105]. Similarly, the concentration of thermal stresses can cause cracking in the matrix resulting in deterioration of effective load bearing area [17]. GNMPs mitigate the thermal stresses by maintaining the temperature uniformity in the concrete matrix due to their higher thermal conductivity [43,106]. Moreover, higher aspect ratio plated structure enable them to block and divert the micro-cracks, resulting in slowing down crack progression which is reflected in their higher strain taking capability [106].



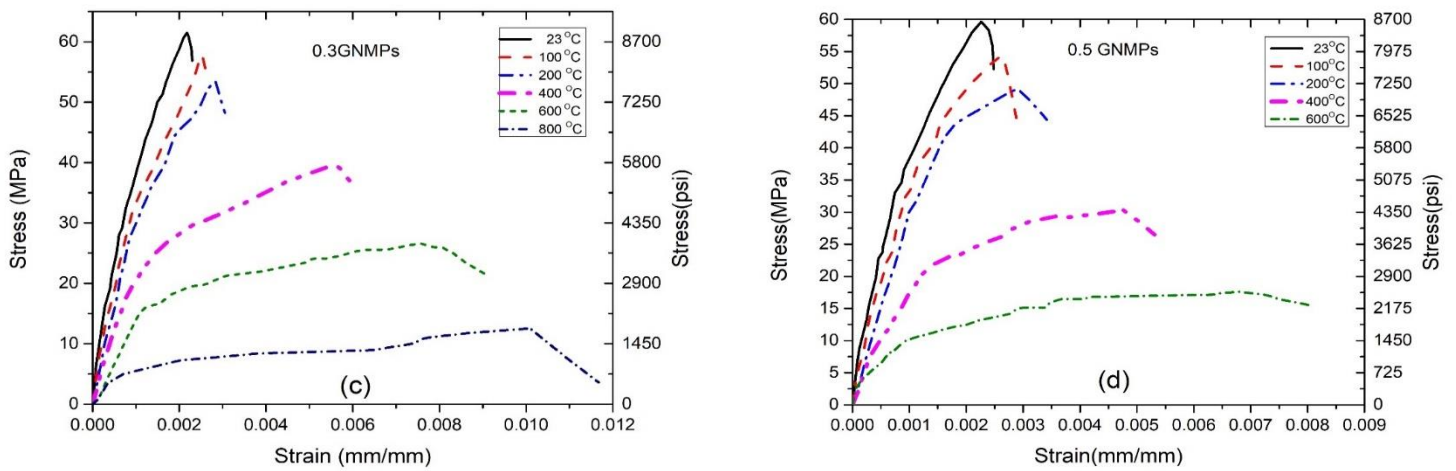


Figure 24 : Residual stress-strain response at ambient and elevated targeted temperatures of analyzed formulations a) HSC b) 0.1GNMPs c) 0.3GNMPs d) 0.5GNMPs

4.4.2 Stress strain response for rapid cooling/quenching method

The peak strain values for HSC were 20%, 33%, 101% and 173% higher after exposure to 100, 200, 400 and 600°C, as compared to the ambient temperature strains as shown in Figure 26. For 0.1GNMPs, the peak strain values were 11%, 45%, 96%, 176% and 281% at 100, 200, 400, 600 and 800°C, as compared to ambient temperature strain. For 0.3GNMPs, the peak strain values were 26%, 59%, 141%, 231% and 327% after exposure to 100, 200, 400 and 600 and 800°C as compared to ambient temperature strain. The peak strain values for 0.5GNMPs were 11%, 30%, 86% and 193% higher after exposure to 100, 200, 400 and 600°C as compared with ambient temperature strain. Peak values of stress and strains were greater for 0.3GNMPs due to sufficient quantity and uniform distribution of GNMPs in the modified mix. As compared to residual method, rapid cooling causes lower peak stresses and strains due to additional thermal stresses developed by sudden cooling of specimens by water spraying.

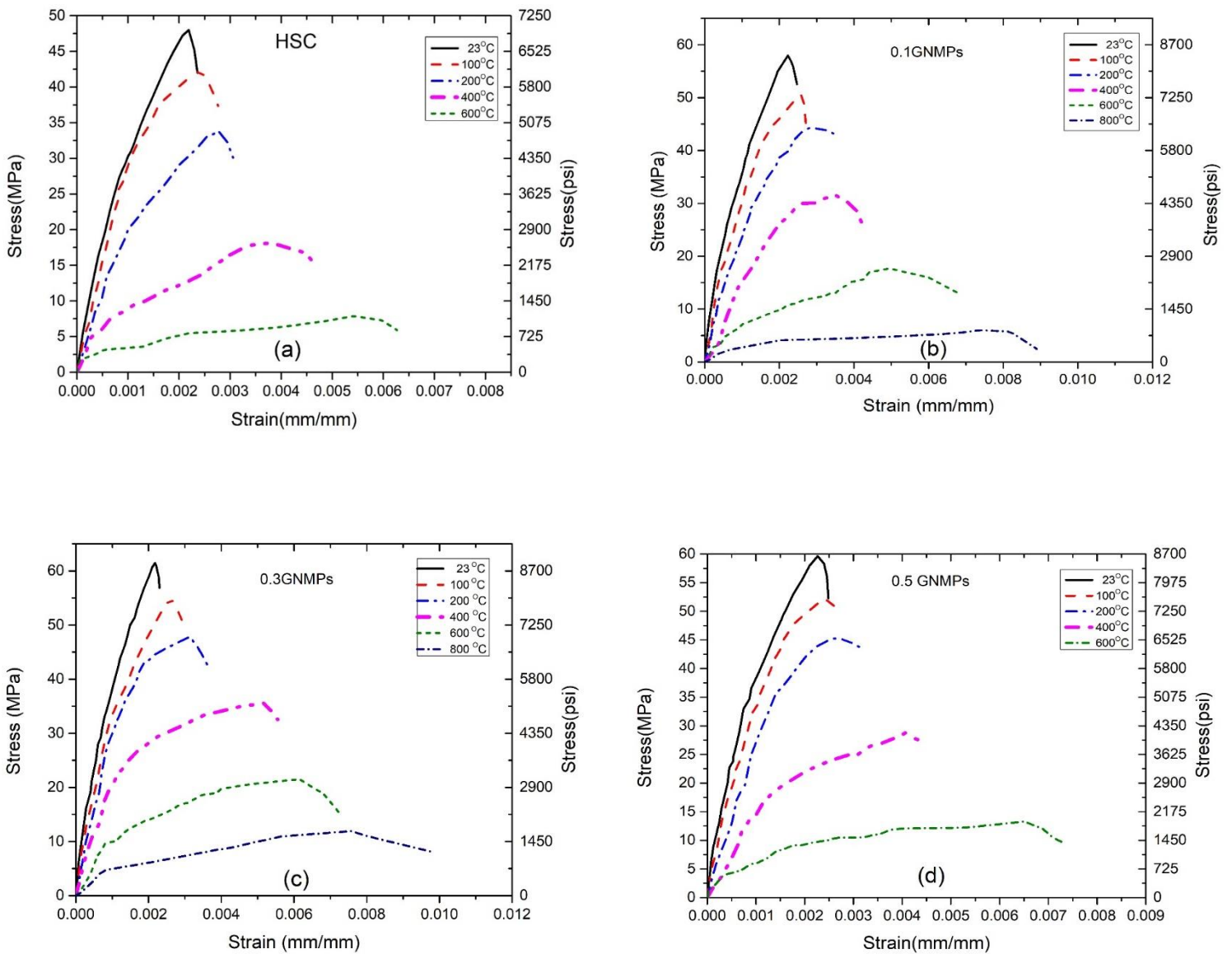


Figure 25 : Stress-strain response at ambient and elevated targeted temperature of analyzed formulation (rapid cooling/quenching method) a) HSC b) 0.1GNMPs c) 0.3GNMPs d) 0.5GNMPs

4.5 Modulus of elasticity

For all the mix samples elastic modulus was evaluated at strains that corresponds to 40% of the values of stress at each of the targeted temperature.

4.5.1 Residual modulus of elasticity

Elastic modulus for all concrete types was calculated as per the procedure given in ASTM C469/C469M-14 [97]. For all the analyzed mixtures, elastic modulus was evaluated at strains corresponding to 40% of the values of stress at each of the targeted temperature. The results are demonstrated in the form of absolute (E_T) and relative (E_T/E) loss of elastic modulus in Figure 27 and 28. GNMPs concrete showed higher elastic modulus than the HSC mix. The enhancement in strength and modulus could be associated with greater strength and greater aspect ratio of the graphite platelets along with the homogeneous dispersion and favorable interfacial bonding between the matrix and added platelets [32,52]. Aforementioned characteristics add valuable transfer of load from the matrix to the platelets [35]. It can also be seen that the modulus of elasticity continued to decrease by increasing the temperature accompanying the deficit of only 12% at 100°C for 0.3GNMPs and the loss was almost 23% at 200°C. The loss in modulus at 400°C for HSC, 0.1GNMPs, 0.3GNMPs and 0.5GNMPs were recorded as 61%, 49%, 45% and 53% respectively. While the loss in modulus at 600°C for HSC, 0.1GNMPs, 0.3GNMPs and 0.5GNMPs were 91%, 77%, 66% and 79% respectively, as compared to that of room temperature.

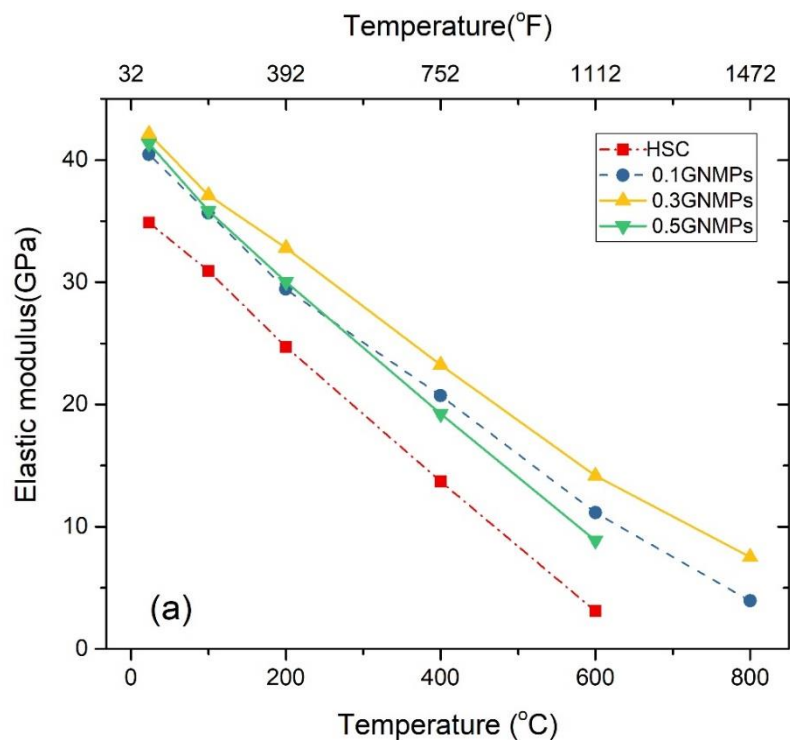


Figure 26 : Variation in absolute residual modulus of elasticity of HSC and nano/micro graphite platelets modified HSC at ambient and elevated temperatures

The loss in modulus of HSC was 61% and 91%, while in 0.3GNMPs the loss was 45% and 66% at 400 and 600°C, respectively, which showed relatively better performance of modified samples. Smaller size particles enables GNMPs to serve as nuclei which can improve the homogeneity and compactness of cement matrix [106]. The loss of modulus in 0.3GNMPs was 45% and 66% at 400 and 600°C, while 0.5GNMPs showed loss of 53% and 79% respectively. Similarly, 0.3GNMPs showed relatively better performance than 0.1GNMPs and loss in modulus was 82% at 800°C as compared to loss of 90% in 0.1GNMPs. Due to uniform dispersion and adequate quantity of GNMPs in 0.3GNMPs, thermal stresses were quite well scattered [43]. So, 0.3GNMPs showed better performance to retain the loss in elastic modulus at elevated temperatures in comparison to remaining formulation.

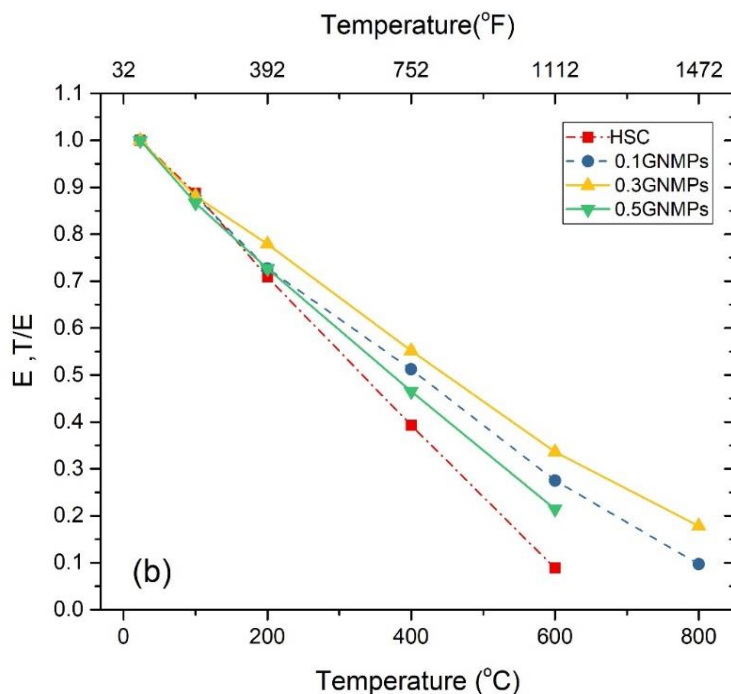


Figure 27 : Variation in relative residual modulus of elasticity of HSC and nano/micro graphite platelets modified HSC at ambient and elevated temperatures

4.5.2 Modulus of elasticity for rapid cooling/quenching method

GNMPs have greater influence on the elastic modulus at elevated temperatures. The loss in modulus of elasticity at 100°C was almost 15%-17% for all composites as shown in Figure 29 and 30. But with further increase in temperature loss was greater in HSC. At 400°C loss in modulus for HSC, 0.1 GNMPs, 0.3 GNMPs, 0.5 GNMPs were 67%, 60%, 51%, 61% while at 600°C the losses were 92%, 82%, 72%, 87%. 0.3 GNMPs shows maximum resistance against

elevated temperature. Higher loss in elastic modulus was occurred in fast cooling method due to thermal shocks generated by water spraying on the heated samples.

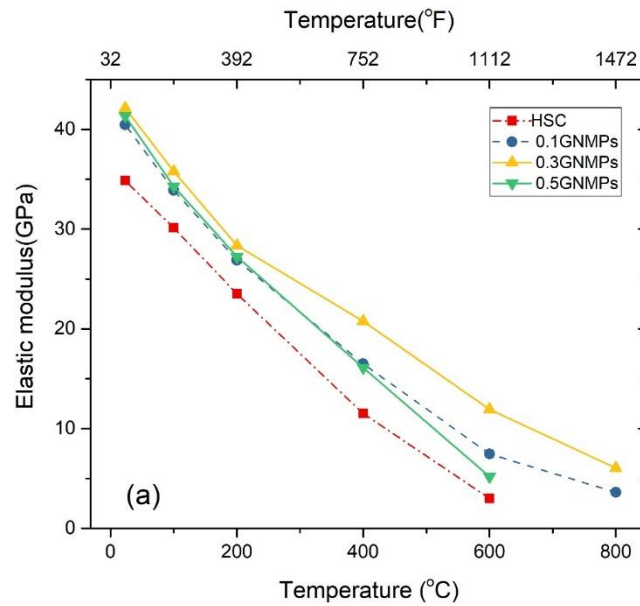


Figure 28 : Variation in relative modulus of elasticity of HSC and nano/micro graphite platelets modified HSC at ambient and elevated temperatures (fast cooling/quenching method)

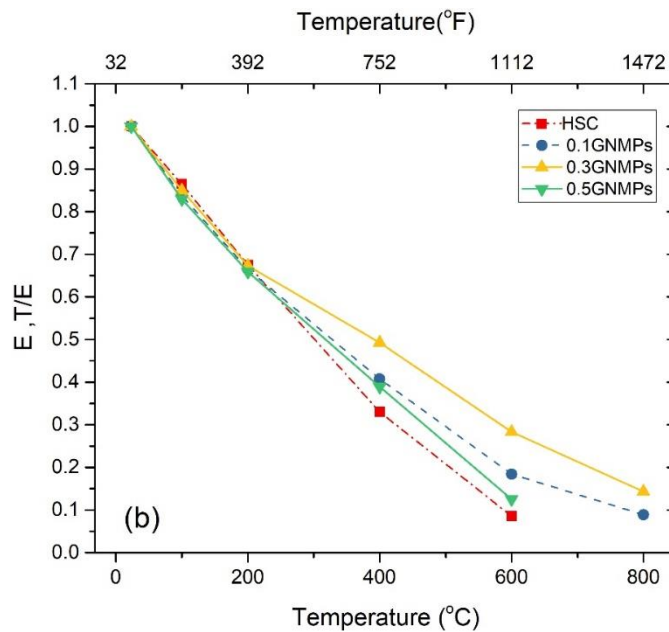


Figure29: Variation in relative modulus of elasticity of HSC and nano/micro graphite platelets modified HSC at ambient and elevated temperatures (fast cooling/quenching method)

4.6 Ultrasonic pulse velocity test

To get an understanding about the serviceability and quality of the analyzed specimens, ultrasonic pulse velocity (UPV) test was conducted before and after exposure to targeted temperature as per ASTM C597 procedure [107].

4.6.1 Residual Ultrasonic pulse velocity

UPV test was performed for determining the extent of fire damage. A higher severity of damage is associated with smaller value of UPV. Figure 31 shows that the GNMPs concretes owe higher values of UPV compared with the reference HSC mix that may be attributed to the development of relatively lesser cracks. Because of lower thermal conductivity of concrete, thermal stresses are not very well scattered that contributes in the formation of concentrated stress pockets [43]. 0.3GNMPs exhibited highest values of UPV due to optimum amount and uniform distribution of graphite nano/micro platelet which are deemed useful as per the mechanical tests. These platelets act as effective heat carrier and uniformly distribute the heat in the matrix due to higher thermal conductivity and reduce the thermal cracking by scattering the thermal stresses. 0.1% GNMPs mix was insufficient to cater for the mitigation of micro-cracking and hence the value of pulse velocity was lower as compared to 0.3% GNMPs mix. 0.5 GNMPs performed better than HSC. However, due to the agglomeration of highly stiffed platelets, concentrated cracks were developed and hence the UPV value of 0.5GNMPs was relatively lower as compared to 0.3GNMPs mix [23].

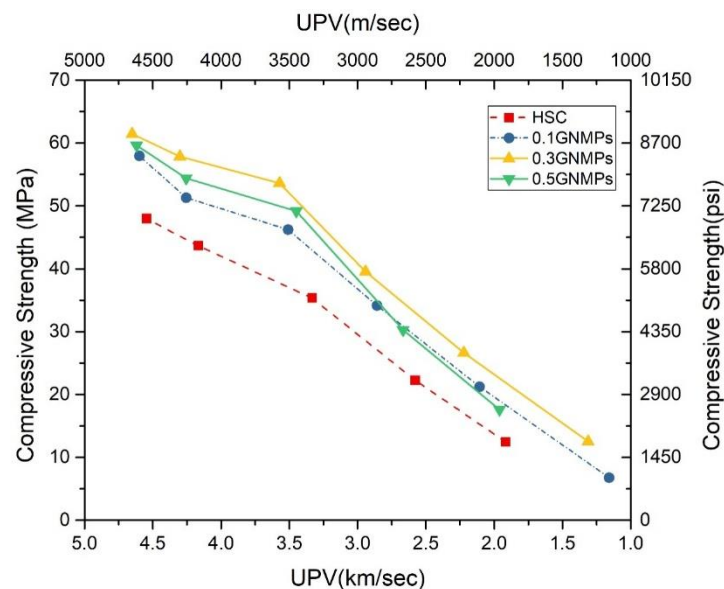


Figure 30: Variation in residual UPV of HSC and nano/micro graphite platelets modified HSC at ambient and elevated temperatures

4.6.2 Ultrasonic pulse velocity for rapid cooling/quenching method

The smaller values of UPV is associated with higher severity of damage. Figure 32 shows that the GNMPs concrete has higher value of UPV. This can be associated to the filler effect of GNMPs. Moreover, for HSC the decrease in UPV values was higher as compared to GNMPs concrete because of the more cracks developed in HSC as compared to GNMPs concrete. 0.3GNMPs exhibited highest values of UPV due to sufficient amount and uniform distribution of graphite nano/micro platelets. 0.1% of nano/micro platelets were insufficient to release vapor pressure from core of concrete that lead to micro-cracks and hence the value of pulse velocity was lower as compared to 0.3% GNMPs mix.

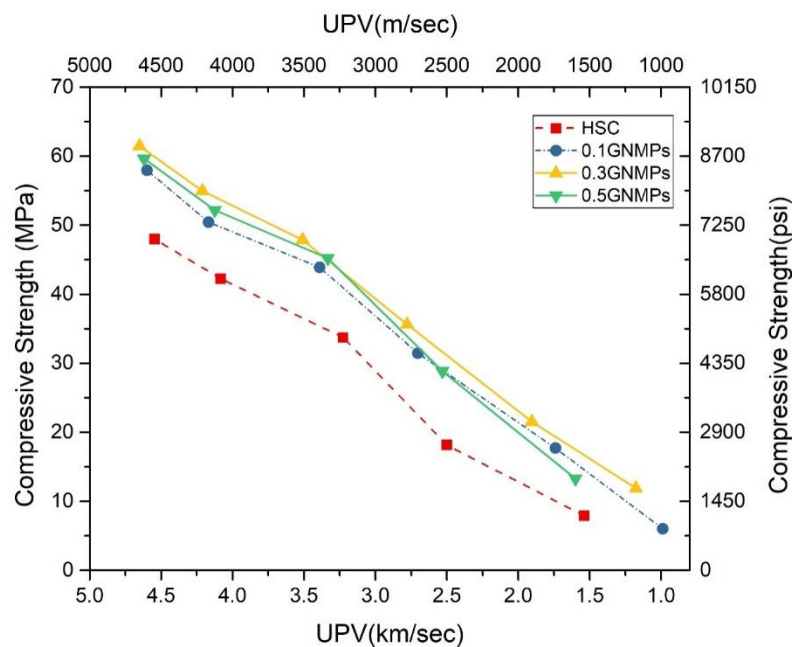


Figure 31: Variation in UPV of HSC and nano/micro graphite platelets modified HSC at ambient and elevated temperatures (Rapid cooling/quenching method)

4.7 Mass loss

All concrete samples lost some mass when exposed to elevated temperatures. Concrete as a hydrated bonding matrix holds a balance between the mass loss and concrete strength due to the disturbances in the associated moisture. Since the mixing of water with concrete plays an important role in hydrating cement and strength development, the moisture loss affects strength and degradation of the concrete mix. At high temperature water expels at pressure which causes cracking in matrix as well [77]. Thus, the loss of mass at higher temperatures is associated to

the loss of moisture and hence bears a direct relation with the concrete strength. Dehydration of hydrated chemical compounds (like calcium hydroxide and C-S-H gel) in the concrete also takes place at the temperatures higher than 400°C and results in a loss of overall concrete mass.

4.7.1 Residual Mass loss

Figure 33 shows the relative mass loss of the analyzed formulations. The average mass loss at 200°C and 400°C was almost 2% and 5%, respectively for all the concrete mixtures. The observed mass loss in 0.1GNMPs at 800°C was 11%, while the loss was 10% in 0.3GNMPs. Mass loss of HSC was 6% and 8.3%, while in 0.3GNMPs the mass loss was 4.3% and 7% at 400°C and 600°C, respectively. The observed pattern of results conforms to the previous study on high performance concrete by Huzeyfa and Nilufer [72]. Mass loss in HSC was more than the mass loss in GNMPs modified mix which may be associated to the refined pore structure of GNMPs formulations at ambient conditions [108]. Nano size effect, enable GNMPs to serve as nuclei that accelerate the hydration reaction of cementitious composites and reduce the porosity of concrete [52]. Due to large surface area more hydrates are formed on the surface of GNMPs and high density CSH gel is produced. This high-density gel increases the temperature exposure range of evaporable liquid making difficult for the water to expel it from the matrix and hence less mass loss occur in GNMPs concrete as compared to reference HSC mix.

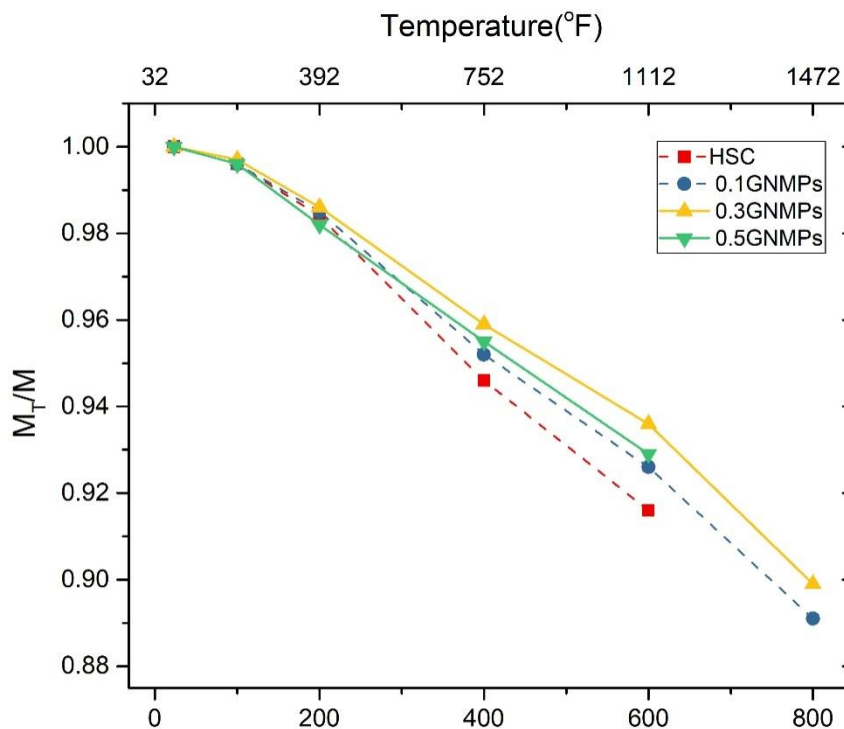


Figure 32 : Residual relative decrease in mass of HSC and nano/micro graphite platelets modified HSC at ambient and elevated temperatures

4.7.2 Mass loss for rapid cooling/quenching method

All the samples loss mass upon exposure to fire. Dehydration of hydrated chemical compounds (like calcium hydroxide and C-S-H gel) in concrete occurs at elevated temperature which causes a loss in mass of concrete. The decrease in the mass is shown in Figure 34. The mass loss at 400°C was almost 5% and at 600°C was 9%. The mass loss in 0.5GNMPs at 800°C was 11.5% and in 0.1GNMPs the loss was 12%. Mass loss in HSC was more than the mass loss in GNMPs due to high porosity of HSC as compared to GNMPs. Nano/micro platelets of GNMPs have dense microstructure and showed lesser mass loss as compared to HSC.

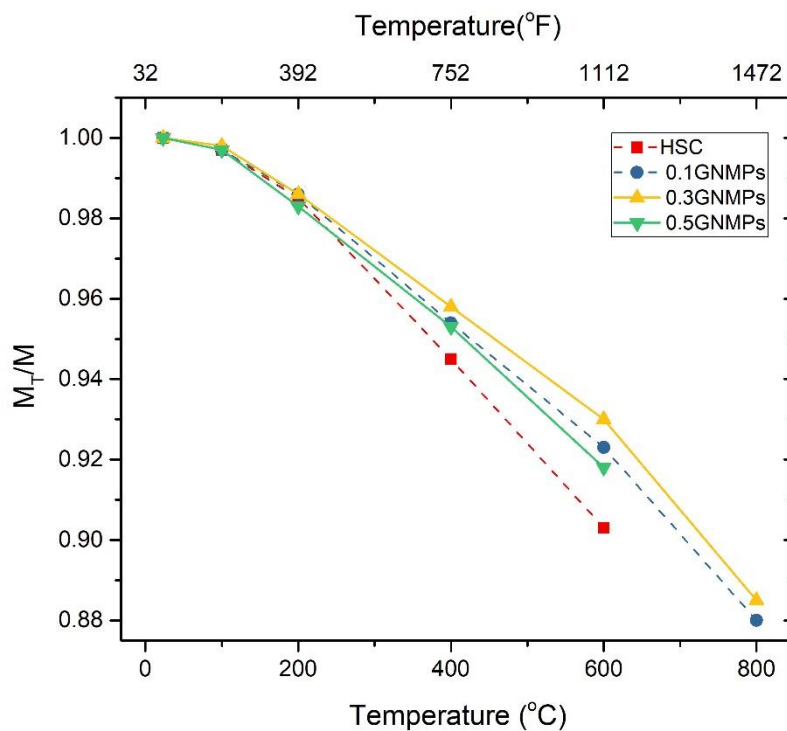


Figure 33 : Relative decrease in mass of HSC and nano/micro graphite platelets modified HSC at ambient and elevated temperatures (Rapid cooling/quenching method)

4.8 Mathematical relationships

Mathematical equations have been developed with the accumulated data for residual and fast cooling test conditions over complete range of temperature between 23-800°C. These mathematical equations might help to estimate the post fire residual capacity of damaged structural member. The mentioned relationships are established employing linear regression, using a commercial software Minitab [109]. Each analytical design was achieved by using

material property as the response variable and temperature as the predictor. The coefficient of determination (R^2) determines the efficiency of an analytical model. The coefficients for the present study lie in the range of 0.85 and 0.99, hence corresponding to a fair comparison of the properties of HSC and GNMPs concrete mixtures.

The alteration of the material properties such as compressive strength ($f'_{c,T}$), splitting tensile strength ($f'_{t,T}$), ultrasonic pulse velocity (UPV), elastic modulus (ET) and mass loss (MT) corresponding to temperature can be associated by a coefficient β_T . The coefficient β_T correlates the value of investigated parameters ($f'_{c,T}$, $f'_{t,T}$, UPV, ET, and MT) at targeted high temperature with reference to their values in ambient conditions. The relationships are summarized in Table 7 and 8 for the residual and fast cooling techniques in physical and mechanical domains limited to the defined temperature range. The reduction factor β_T at various temperatures may evaluate splitting tensile and compressive strength, modulus of elasticity, and mass loss for the investigated formulations.

Table 7 : High temperature material property relations for HSC and nano/micro graphite modified HSC mixtures (Residual test condition).

Formulation	Property Relationship	
HSC	$\beta_{T, \text{compression}} = \{1.0210 - 0.001312T$ $\beta_{T, \text{tensile}} = \{0.9304 - 0.001317T$ $\beta_{T, \text{mass}} = \{1.00896 - 0.000153T$ $\beta_{T, \text{UPV}} = \{0.9938 - 0.001006T$ $\beta_{T, \text{modulus}} = \{1.03623 - 0.001590T$	$23^\circ\text{C} \leq T \leq 600^\circ\text{C}^*\}$ $23^\circ\text{C} \leq T \leq 600^\circ\text{C}^*\}$ $23^\circ\text{C} \leq T \leq 600^\circ\text{C}^*\}$ $23^\circ\text{C} \leq T \leq 600^\circ\text{C}^*\}$ $23^\circ\text{C} \leq T \leq 600^\circ\text{C}^*\}$
	*Specimens spall off beyond 600°C	
0.1GNMPs	$\beta_{T, \text{compression}} = \{1.0178 - 0.001018T$ $\beta_{T, \text{tensile}} = \{0.9655 - 0.001189T$ $\beta_{T, \text{mass}} = \{1.00897 - 0.000143T$ $\beta_{T, \text{UPV}} = \{1.0007 - 0.000935T$ $\beta_{T, \text{modulus}} = \{0.9918 - 0.001158T$	$23^\circ\text{C} \leq T \leq 800^\circ\text{C}$ $23^\circ\text{C} \leq T \leq 800^\circ\text{C}$ $23^\circ\text{C} \leq T \leq 800^\circ\text{C}$ $23^\circ\text{C} \leq T \leq 800^\circ\text{C}$ $23^\circ\text{C} \leq T \leq 800^\circ\text{C}$
0.3GNMPs	$\beta_{T, \text{compression}} = \{1.0495 - 0.001037T$ $\beta_{T, \text{tensile}} = \{1.0063 - 0.001099T$ $\beta_{T, \text{mass}} = \{1.00889 - 0.000130T$ $\beta_{T, \text{UPV}} = \{0.9937 - 0.000895T$ $\beta_{T, \text{modulus}} = \{0.9956 - 0.001059T$	$23^\circ\text{C} \leq T \leq 800^\circ\text{C}$ $23^\circ\text{C} \leq T \leq 800^\circ\text{C}$ $23^\circ\text{C} \leq T \leq 800^\circ\text{C}$ $23^\circ\text{C} \leq T \leq 800^\circ\text{C}$ $23^\circ\text{C} \leq T \leq 800^\circ\text{C}$

0.5GNMPs	$\beta_{T, \text{compression}} = \{1.0411 - 0.001258T \quad 23^{\circ}\text{C} \leq T \leq 600^{\circ}\text{C}^*\}$
	$\beta_{T, \text{tensile}} = \{0.9997 - 0.001300T \quad 23^{\circ}\text{C} \leq T \leq 600^{\circ}\text{C}^*\}$
	$\beta_{T, \text{mass}} = \{1.00611 - 0.000127T \quad 23^{\circ}\text{C} \leq T \leq 600^{\circ}\text{C}^*\}$
	$\beta_{T, \text{UPV}} = \{0.9991 - 0.001002T \quad 23^{\circ}\text{C} \leq T \leq 600^{\circ}\text{C}^*\}$
	$\beta_{T, \text{modulus}} = \{1.0102 - 0.001344T \quad 23^{\circ}\text{C} \leq T \leq 600^{\circ}\text{C}^*\}$
*Specimens spall off beyond 600°C	

Table 8 : High temperature material property relations for HSC and nano/micro modified HSC mixtures (Rapid cooling method/quenching method).

Formulation	Property Relationship
HSC	$\beta_{T, \text{compression}} = \{1.0159 - 0.001446T \quad 23^{\circ}\text{C} \leq T \leq 600^{\circ}\text{C}^*\}$ $\beta_{T, \text{tensile}} = \{0.9228 - 0.001446 T \quad 23^{\circ}\text{C} \leq T \leq 600^{\circ}\text{C}^*\}$ $\beta_{T, \text{mass}} = \{1.01223 - 0.000175 T \quad 23^{\circ}\text{C} \leq T \leq 600^{\circ}\text{C}^*\}$ $\beta_{T, \text{UPV}} = \{0.9960 - 0.001122 T \quad 23^{\circ}\text{C} \leq T \leq 600^{\circ}\text{C}^*\}$ $\beta_{T, \text{modulus}} = \{1.0160 - 0.001606 T \quad 23^{\circ}\text{C} \leq T \leq 600^{\circ}\text{C}^*\}$ *Specimens spall off beyond 600°C
0.1GNMPs	$\beta_{T, \text{compression}} = \{0.9985 - 0.001136 T \quad 23^{\circ}\text{C} \leq T \leq 800^{\circ}\text{C}\}$ $\beta_{T, \text{tensile}} = \{0.92411 - 0.001139 T \quad 23^{\circ}\text{C} \leq T \leq 800^{\circ}\text{C}\}$ $\beta_{T, \text{mass}} = \{1.01190 - 0.000156 T \quad 23^{\circ}\text{C} \leq T \leq 800^{\circ}\text{C}\}$ $\beta_{T, \text{UPV}} = \{0.9904 - 0.001122 T \quad 23^{\circ}\text{C} \leq T \leq 800^{\circ}\text{C}\}$ $\beta_{T, \text{modulus}} = \{0.9478 - 0.001179 T \quad 23^{\circ}\text{C} \leq T \leq 800^{\circ}\text{C}\}$
0.3GNMPs	$\beta_{T, \text{compression}} = \{1.0011 - 0.001041 T \quad 23^{\circ}\text{C} \leq T \leq 800^{\circ}\text{C}\}$ $\beta_{T, \text{tensile}} = \{0.9925 - 0.001145 T \quad 23^{\circ}\text{C} \leq T \leq 800^{\circ}\text{C}\}$ $\beta_{T, \text{mass}} = \{1.01174 - 0.000148 T \quad 23^{\circ}\text{C} \leq T \leq 800^{\circ}\text{C}\}$ $\beta_{T, \text{UPV}} = \{0.9904 - 0.000998 T \quad 23^{\circ}\text{C} \leq T \leq 800^{\circ}\text{C}\}$ $\beta_{T, \text{modulus}} = \{0.9540 - 0.001075 T \quad 23^{\circ}\text{C} \leq T \leq 800^{\circ}\text{C}\}$
0.5GNMPs	$\beta_{T, \text{compression}} = \{0.9847 - 0.001410 T \quad 23^{\circ}\text{C} \leq T \leq 600^{\circ}\text{C}^*\}$ $\beta_{T, \text{tensile}} = \{0.9857 - 0.001393 T \quad 23^{\circ}\text{C} \leq T \leq 600^{\circ}\text{C}^*\}$ $\beta_{T, \text{mass}} = \{1.00894 - 0.000146 T \quad 23^{\circ}\text{C} \leq T \leq 600^{\circ}\text{C}^*\}$ $\beta_{T, \text{UPV}} = \{0.9956 - 0.001110 T \quad 23^{\circ}\text{C} \leq T \leq 600^{\circ}\text{C}^*\}$ $\beta_{T, \text{modulus}} = \{1.0215 - 0.001374 T \quad 23^{\circ}\text{C} \leq T \leq 600^{\circ}\text{C}^*\}$ *Specimens spall off beyond 600°C

5 Conclusions

The results provided in this study report new data on fire endurance of concretes containing graphite nano/micro platelets and were compared with well-established data of high strength concretes (HSCs). Variable amount of GNMPs were used i.e. 0.1, 0.3 and 0.5%. Optimum dosage of GNMPs in high strength concrete at elevated temperatures is conclusively believed as 0.3%. Based on the results obtained in this study following conclusions are drawn:

- i. The presence of graphite nano/micro platelets improve the compressive strength of samples pre and post-fire exposure. GNMPs modified high strength concrete samples exhibit lower strength degradation due to their thermally efficient behavior that scatters the thermal stresses in effective way.
- ii. Graphite nano/micro platelets contribute in adding the splitting tensile strength of modified mixes as they effectively delay the initiation and progression phases of cracks.
- iii. Stress-strain response shows reduced strength loss and increased peak and rupture strain at both ambient and elevated temperatures for graphite nano/micro platelets modified high strength concretes.
- iv. Graphite nano/micro platelets modified high strength concrete formulations owe better mass retention at high temperature because of the filler effect of GNMPs leading to refinement of pores.
- v. GNMPs modified samples show higher ultrasonic pulse velocity values as compared to the control samples, indicating less damage and less internal cracks after fire exposure.
- vi. GNMPs modified mixtures show high modulus of elasticity because of higher modulus of graphite nano/micro platelets.
- vii. 0.3% GNMPs showed better physical and mechanical properties as compared to other GNMPs formulations indicating the optimum dosage of GNMPs in high strength concrete at elevated temperature to be 0.3%.
- viii. Quick/Rapid cooling produce higher loss in concrete properties than slow cooling because quick cooling produces thermal shock in concrete resulting in temperature differential between the outer and inner layers of concrete.

- ix. Mathematical models are proposed for material fire performance of the GNMPs modified high strength concrete formulation in the investigated temperature zone ranging between 23 till 800°C.

Recommendations

1. Stressed and unstressed properties should be checked.
2. A complete investigation of structural behavior should be studied for members made up of GNMPs concrete.
3. Use of other carbonaceous nano material like CNT or CNF along with GNMPs and their effect on fire performance.

6 References

- [1] S. Hun, D. Joo, G. Sung, K. Taek, Cement & Concrete Composites Tensile behavior of Ultra High Performance Hybrid Fiber Reinforced Concrete, Cement and Concrete Composites. 34 (2012) 172–184. doi:10.1016/j.cemconcomp.2011.09.009.
- [2] W. Meng, K.H. Khayat, Experimental and numerical studies on flexural behavior of ultra-high-performance concrete panels reinforced with embedded glass fiber-reinforced polymer grids, Transportation Research Record. 2592 (2016) 38–44. doi:10.3141/2592-05.
- [3] K. Wille, D.J. Kim, A.E. Naaman, Strain-hardening UHP-FRC with low fiber contents, Materials and Structures/Materiaux et Constructions. 44 (2011) 583–598. doi:10.1617/s11527-010-9650-4.
- [4] A.M. Neville, Properties of Concrete, 2011. doi:10.4135/9781412975704.n88.
- [5] N. Amarkhail, Effects of Silica Fume on Properties of High-Strength Concrete, International Journal of Technical Research and Applications. 6 (2015) 13–19.
- [6] M. Mazloom, A.A. Ramezaniapour, J.J. Brooks, Effect of silica fume on mechanical properties of high-strength concrete, Cement and Concrete Composites. 26 (2004) 347–357. doi:10.1016/S0958-9465(03)00017-9.
- [7] K. Sakr, E. El-Hakim, Effect of high temperature or fire on heavy weight concrete properties, Cement and Concrete Research. 35 (2005) 590–596. doi:10.1016/j.cemconres.2004.05.023.
- [8] K.D. Hertz, Concrete strength for fire safety design, Magazine of Concrete Research. 57 (2005) 445–453.
- [9] G.A. Khoury, C.E. Majorana, F. Pesavento, B.A. Schrefler, Modelling of heated concrete, Magazine of Concrete Research. 54 (2002) 77–101. doi:10.1680/macr.54.2.77.40895.
- [10] K.D. Hertz, L.S. Sørensen, Test method for spalling of fire exposed concrete, Fire Safety Journal. 40 (2005) 466–476. doi:10.1016/j.firesaf.2005.04.001.
- [11] B.M. Luccioni, M.I. Figueroa, R.F. Danesi, Thermo-mechanic model for concrete exposed to elevated temperatures, Engineering Structures. 25 (2003) 729–742. doi:10.1016/S0141-0296(02)00209-2.

- [12] O.A. Ã, O. Arioz, Effects of elevated temperatures on properties of concrete, *Fire Safety Journal*. 42 (2007) 516–522. doi:10.1016/j.firesaf.2007.01.003.
- [13] L.T. Phan, J.R. Lawson, F.L. Davis, Effects of elevated temperature exposure on heating characteristics, spalling, and residual properties of high performance concrete, *Materials and Structures*. 34 (2001) 83–91. doi:10.1007/BF02481556.
- [14] P. Kalifa, F.D. Menneteau, D. Quenard, Spalling and pore pressure in HPC at high temperatures, *Cement and Concrete Research*. 30 (2000) 1915–1927. doi:10.1016/S0008-8846(00)00384-7.
- [15] R. Kowalski, Mechanical properties of concrete subjected to high temperature, *Architecture Civil Engineering Environment*. (2010) 61–70.
- [16] P. Kalifa, G. Chén , C. Gall , High-temperature behavior of HPC with polypropylene fibers from spalling to microstructure, *Cement and Concrete Research*. 31 (2001) 1487–1499.
- [17] A. Behnood, M. Ghandehari, Comparison of compressive and splitting tensile strength of high-strength concrete with and without polypropylene fibers heated to high temperatures, *Fire Safety Journal*. 44 (2009) 1015–1022. doi:10.1016/j.firesaf.2009.07.001.
- [18] S.L. Suhaendi, T. Horiguchi, Fiber-reinforced high-strength concrete under elevated temperature-effect of fibers on residual properties, in: *Fire Safety Science*, 2005: pp. 271–278. doi:10.3801/IAFSS.FSS.8-271.
- [19] H. Caetano, G. Ferreira, J. Paulo, C. Rodrigues, P. Pimenta, Effect of the high temperatures on the microstructure and compressive strength of high strength fibre concretes, *Construction and Building Materials*. 199 (2019) 717–736. doi:10.1016/j.conbuildmat.2018.12.074.
- [20] C. Li, D. Gao, Y. Wang, J. Tang, Effect of high temperature on the bond performance between basalt fibre reinforced polymer (BFRP) bars and concrete, *Construction and Building Materials*. 141 (2017) 44–51. doi:10.1016/j.conbuildmat.2017.02.125.
- [21] F.B. Varona, F.J. Baeza, D. Bru, S. Ivorra, Evolution of the bond strength between reinforcing steel and fibre reinforced concrete after high temperature exposure, *Construction and Building Materials*. 176 (2018) 359–370. doi:10.1016/j.conbuildmat.2018.05.065.

- [22] J. Li, M.L. Sham, J.K. Kim, G. Marom, Morphology and properties of UV/ozone treated graphite nanoplatelet/epoxy nanocomposites, *Composites Science and Technology*. 67 (2007) 296–305. doi:10.1016/j.compscitech.2006.08.009.
- [23] S. Chandrasekaran, C. Seidel, K. Schulte, Preparation and characterization of graphite nano-platelet (GNP)/epoxy nano-composite: Mechanical, electrical and thermal properties, *European Polymer Journal*. 49 (2013) 3878–3888. doi:10.1016/j.eurpolymj.2013.10.008.
- [24] K. Kalaitzidou, H. Fukushima, L.T. Drzal, Multifunctional polypropylene composites produced by incorporation of exfoliated graphite nanoplatelets, *Carbon*. 45 (2007) 1446–1452. doi:10.1016/j.carbon.2007.03.029.
- [25] W.L. Baloch, R.A. Khushnood, W. Khaliq, Influence of multi-walled carbon nanotubes on the residual performance of concrete exposed to high temperatures, *Construction and Building Materials*. 185 (2018) 44–56. doi:10.1016/j.conbuildmat.2018.07.051.
- [26] A. Peyvandi, L.A. Sbia, P. Soroushian, K. Sobolev, Effect of the cementitious paste density on the performance efficiency of carbon nanofiber in concrete nanocomposite, *Construction and Building Materials*. 48 (2013) 265–269. doi:10.1016/j.conbuildmat.2013.06.094.
- [27] H. SIXUAN, Multifunctional graphite nanoplatelets (GNP) reinforced cementitious composites Huang Sixuan (B . Eng ., Tsinghua University), (2012) 152.
- [28] W.L. Baloch, R.A. Khushnood, S.A. Memon, W. Ahmed, S. Ahmad, Effect of Elevated Temperatures on Mechanical Performance of Normal and Lightweight Concretes Reinforced with Carbon Nanotubes, *Fire Technology*. 54 (2018) 1331–1367. doi:10.1007/s10694-018-0733-z.
- [29] L. Ahmed Sbia, A. Peyvandi, P. Soroushian, J. Lu, A.M. Balachandra, Enhancement of Ultrahigh Performance Concrete Material Properties with Carbon Nanofiber, *Advances in Civil Engineering*. 2014 (2014). doi:10.1155/2014/854729.
- [30] G.Y. Li, P.M. Wang, X. Zhao, Mechanical behavior and microstructure of cement composites incorporating surface-treated multi-walled carbon nanotubes, *Carbon*. 43 (2005) 1239–1245. doi:10.1016/j.carbon.2004.12.017.
- [31] S. Musso, J. Tulliani, G. Ferro, A. Tagliaferro, Influence of carbon nanotubes structure

- on the mechanical behavior of cement composites, *Composites Science and Technology*. 69 (2009) 1985–1990. doi:10.1016/j.compscitech.2009.05.002.
- [32] W. Meng, K.H. Khayat, Effect of graphite nanoplatelets and carbon nanofibers on rheology, hydration, shrinkage, mechanical properties, and microstructure of UHPC, *Cement and Concrete Research*. 105 (2018) 64–71. doi:10.1016/j.cemconres.2018.01.001.
- [33] L.M. Viculis, J.J. Mack, O.M. Mayer, H.T. Hahn, R.B. Kaner, Intercalation and exfoliation routes to graphite nanoplatelets, *Journal of Materials Chemistry*. 15 (2005) 974–978. doi:10.1039/b413029d.
- [34] Y. Gao, O.T. Picot, H. Zhang, E. Bilotti, T. Peijs, Synergistic effects of filler size on thermal annealing-induced percolation in polylactic acid (PLA)/graphite nanoplatelet (GNP) nanocomposites, *Nanocomposites*. 3 (2017) 67–75. doi:10.1080/20550324.2017.1333780.
- [35] A. Yasmin, I.M. Daniel, Mechanical and thermal properties of graphite platelet/epoxy composites, *Polymer*. 45 (2004) 8211–8219. doi:10.1016/j.polymer.2004.09.054.
- [36] B. Li, W.H. Zhong, Review on polymer/graphite nanoplatelet nanocomposites, *Journal of Materials Science*. 46 (2011) 5595–5614. doi:10.1007/s10853-011-5572-y.
- [37] B. Han, S. Sun, S. Ding, L. Zhang, X. Yu, J. Ou, Composites : Part A Review of nanocarbon-engineered multifunctional cementitious composites, *COMPOSITES PART A*. 70 (2015) 69–81. doi:10.1016/j.compositesa.2014.12.002.
- [38] A. Peyvandi, P. Soroushian, A.M. Balachandra, K. Sobolev, Enhancement of the durability characteristics of concrete nanocomposite pipes with modified graphite nanoplatelets, *Construction and Building Materials*. 47 (2013) 111–117. doi:10.1016/j.conbuildmat.2013.05.002.
- [39] L.T. Phan, N.J. Carino, Fire performance of high strength concrete: Research needs, in: *Structures Congress 2000: Advanced Technology in Structural Engineering*, 2004. doi:10.1061/40492(2000)181.
- [40] I. Janotka, T. Nürnbergerová, Effect of temperature on structural quality of the cement paste and high-strength concrete with silica fume, *Nuclear Engineering and Design*. 235 (2005) 2019–2032. doi:10.1016/j.nucengdes.2005.05.011.
- [41] W. Khaliq, Mechanical and physical response of recycled aggregates high-strength

- concrete at elevated temperatures, *Fire Safety Journal*. 96 (2018) 203–214.
doi:10.1016/j.firesaf.2018.01.009.
- [42] M.I. Mousa, Effect of elevated temperature on the properties of silica fume and recycled rubber-filled high strength concretes (RHSC), *HBRC Journal*. 13 (2017) 1–7.
doi:10.1016/j.hbrcj.2015.03.002.
- [43] X. Cui, S. Sun, B. Han, X. Yu, J. Ouyang, S. Zeng, J. Ou, Mechanical, thermal and electromagnetic properties of nanographite platelets modified cementitious composites, *Composites Part A: Applied Science and Manufacturing*. 93 (2017) 49–58. doi:10.1016/j.compositesa.2016.11.017.
- [44] N. Grobert, Carbon nanotubes – importance of clean CNT material for the success of future applications ., *Materials Today*. 10 (2007) 28–35. doi:10.1016/S1369-7021(06)71789-8.
- [45] O. Concrete, T.P. Doi, Concrete pavement prediction life model based on electrical response of concrete - CNTs sensors under fatigue loading, (2018).
doi:10.6092/polito/porto/2687875.
- [46] R. Sengupta, M. Bhattacharya, S. Bandyopadhyay, A.K. Bhowmick, A review on the mechanical and electrical properties of graphite and modified graphite reinforced polymer composites, *Progress in Polymer Science (Oxford)*. 36 (2011) 638–670.
doi:10.1016/j.progpolymsci.2010.11.003.
- [47] Z. Anwar, A. Kausar, B. Muhammad, Polymer and Graphite-Derived Nanofiller Composite: An Overview of Functional Applications, *Polymer - Plastics Technology and Engineering*. 55 (2016) 1765–1784. doi:10.1080/03602559.2016.1163598.
- [48] B. Li, W.H. Zhong, B.L.W. Zhong, Review on polymer/graphite nanoplatelet nanocomposites, *Journal of Materials Science*. 46 (2011) 5595–5614.
doi:10.1007/s10853-011-5572-y.
- [49] D. Bansal, S. Pillay, U. Vaidya, Nanographite-reinforced carbon/carbon composites, *Carbon*. 55 (2013) 233–244. doi:10.1016/j.carbon.2012.12.032.
- [50] C. Esposito Corcione, A. Maffezzoli, Transport properties of graphite/epoxy composites: Thermal, permeability and dielectric characterization, *Polymer Testing*. 32 (2013) 880–888. doi:10.1016/j.polymertesting.2013.03.023.
- [51] S. Sun, B. Han, S. Jiang, X. Yu, Y. Wang, H. Li, J. Ou, Nano graphite platelets-

- enabled piezoresistive cementitious composites for structural health monitoring, *Construction and Building Materials*. 136 (2017) 314–328.
doi:10.1016/j.conbuildmat.2017.01.006.
- [52] W. Meng, K.H. Khayat, Mechanical properties of ultra-high-performance concrete enhanced with graphite nanoplatelets and carbon nanofibers, *Composites Part B: Engineering*. 107 (2016) 113–122. doi:10.1016/j.compositesb.2016.09.069.
- [53] A. Nadeem, S. Ali, T. Yiu, The performance of Fly ash and Metakaolin concrete at elevated temperatures, *Construction and Building Materials*. 62 (2014) 67–76.
doi:10.1016/j.conbuildmat.2014.02.073.
- [54] A.S.M.A. Awal, I.A. Shehu, M. Ismail, Effect of cooling regime on the residual performance of high-volume palm oil fuel ash concrete exposed to high temperatures, *CONSTRUCTION & BUILDING MATERIALS*. 98 (2015) 875–883.
doi:10.1016/j.conbuildmat.2015.09.001.
- [55] A.Y. Nassif, S. Rigden, E. Burley, A.S. Rigden, E. Burley, The effects of rapid cooling by water quenching on the stiffness properties of fire-damaged concrete, *Magazine of Concrete* 51 (1999) 255–261. doi:10.1680/mac.1999.51.4.255.
- [56] G.F. Peng, S.H. Bian, Z.Q. Guo, J. Zhao, X.L. Peng, Y.C. Jiang, Effect of thermal shock due to rapid cooling on residual mechanical properties of fiber concrete exposed to high temperatures, *Construction and Building Materials*. 22 (2008) 948–955.
doi:10.1016/j.conbuildmat.2006.12.002.
- [57] N. Amarkhail, High strength Concrete, *International Journal of Technical Research and Applications*, 32 (2015) 13–19.
- [58] ACI 234R-06, 234R-06 Guide for the Use of Silica Fume in Concrete, *Aci 234R-06*. 96 (2006) 0–64.
- [59] M.I. Khan, R. Siddique, Utilization of silica fume in concrete: Review of durability properties, *Resources, Conservation and Recycling*. 57 (2011) 30–35.
doi:10.1016/j.resconrec.2011.09.016.
- [60] Wild, Factors influencing strength development of concrete containing silica fume, *Science*. 25 (1995) 1567–1580.
- [61] H.S. Wong, H.A. Razak, Efficiency of calcined kaolin and silica fume as cement replacement material for strength performance, *Cement and Concrete Research*. 35

- (2005) 696–702. doi:10.1016/j.cemconres.2004.05.051.
- [62] F. Köksal, F. Altun, I. Yiğit, Y. Şahin, Combined effect of silica fume and steel fiber on the mechanical properties of high strength concretes, *Construction and Building Materials*. 22 (2008) 1874–1880. doi:10.1016/j.conbuildmat.2007.04.017.
- [63] A.A. Almusallam, H. Beshr, M. Maslehuddin, O.S.B. Al-Amoudi, Effect of silica fume on the mechanical properties of low quality coarse aggregate concrete, *Cement and Concrete Composites*. 26 (2004) 891–900. doi:10.1016/j.cemconcomp.2003.09.003.
- [64] K.G. Babu, D.S. Babu, Behaviour of lightweight expanded polystyrene concrete containing silica fume, *Cement and Concrete Research*. 33 (2003) 755–762. doi:10.1016/S0008-8846(02)01055-4.
- [65] S. Bhanja, B. Sengupta, Influence of silica fume on the tensile strength of concrete, *Cement and Concrete Research*. 35 (2005) 743–747. doi:10.1016/j.cemconres.2004.05.024.
- [66] E. Güneyisi, M. Gesoğlu, T. Özturan, Properties of rubberized concretes containing silica fume, *Cement and Concrete Research*. 34 (2004) 2309–2317. doi:10.1016/j.cemconres.2004.04.005.
- [67] A.N. Ndoukouo, A. Nubissie, P. Wofo, On the dynamics of fire re-exposed steel beam under mechanical load, *JCSR*. 67 (2011) 1864–1871. doi:10.1016/j.jcsr.2011.05.009.
- [68] S.P. Koganti, S. Sajja, Properties of concrete containing different type of waste materials as aggregate replacement exposed to elevated temperature – A review Properties of concrete containing different type of waste materials as aggregate replacement exposed to elevated temper, *Earth and Environmental Science*. (2018). doi:10.1088/1755-1315/140/1/012139.
- [69] A. Gupta, S. Mandal, S. Ghosh, Recycled aggregate concrete exposed to elevated temperature, *ARPJ Journal of Engineering and Applied Sciences*. 7 (2012) 100–107.
- [70] W. Khaliq, F. Waheed, Mechanical response and spalling sensitivity of air entrained high-strength concrete at elevated temperatures, *Construction and Building Materials*. 150 (2017) 747–757. doi:10.1016/j.conbuildmat.2017.06.039.
- [71] L.T. Phan, N.J. Carino, Effects of Test Conditions and Mixture Proportions on Behavior of High - Strength Concrete Exposed to High Temperatures, *ACI Materials*

- Journal. 99 (2002) 54–66. doi:10.14359/11317.
- [72] A.H. Akca, N.Ö. Zihnioglu, High performance concrete under elevated temperatures, *Construction and Building Materials*. 44 (2013) 317–328. doi:10.1016/j.conbuildmat.2013.03.005.
- [73] M. Bastami, A. Chaboki-Khiabani, M. Baghbadrani, M. Kordi, Performance of high strength concretes at elevated temperatures, *Scientia Iranica*. 18 (2011) 1028–1036. doi:10.1016/j.scient.2011.09.001.
- [74] T. Uygunoğlu, I.B. Topçu, Thermal expansion of self-consolidating normal and lightweight aggregate concrete at elevated temperature, *Construction and Building Materials*. 23 (2009) 3063–3069. doi:10.1016/j.conbuildmat.2009.04.004.
- [75] N. Yüzer, F. Aköz, L.D. Öztürk, Compressive strength-color change relation in mortars at high temperature, *Cement and Concrete Research*. 34 (2004) 1803–1807. doi:10.1016/j.cemconres.2004.01.015.
- [76] A. Behnood, H. Ziari, Effects of silica fume addition and water to cement ratio on the properties of high-strength concrete after exposure to high temperatures, *Cement and Concrete Composites*. 30 (2008) 106–112. doi:10.1016/j.cemconcomp.2007.06.003.
- [77] B. Georgali, P.E. Tsakiridis, Microstructure of fire-damaged concrete. A case study, *Cement and Concrete Composites*. 27 (2005) 255–259. doi:10.1016/j.cemconcomp.2004.02.022.
- [78] Q. Zhou, F.P. Glasser, Thermal stability and decomposition mechanisms of ettringite at 120°C, *Cement and Concrete Research*. 31 (2001) 1333–1339. doi:10.1016/S0008-8846(01)00558-0.
- [79] G.A. Khoury, Compressive strength of concrete at high temperatures: A reassessment, *Magazine of Concrete Research*. 44 (1992) 291–309. doi:10.1680/macr.1992.44.161.291.
- [80] L. Alarcon-Ruiz, G. Platret, E. Massieu, A. Ehrlacher, The use of thermal analysis in assessing the effect of temperature on a cement paste, *Cement and Concrete Research*. 35 (2005) 609–613. doi:10.1016/j.cemconres.2004.06.015.
- [81] H. Tanyildizi, A. Coskun, Performance of lightweight concrete with silica fume after high temperature, *Construction and Building Materials*. 22 (2008) 2124–2129. doi:10.1016/j.conbuildmat.2007.07.017.

- [82] G. Sun, R. Liang, Z. Lu, J. Zhang, Z. Li, Mechanism of cement / carbon nanotube composites with enhanced mechanical properties achieved by interfacial strengthening, *Construction and Building Materials*. 115 (2016) 87–92.
doi:10.1016/j.conbuildmat.2016.04.034.
- [83] J.M. Makar, G.W. Chan, Growth of cement hydration products on single-walled carbon nanotubes, *Journal of the American Ceramic Society*. 92 (2009) 1303–1310.
doi:10.1111/j.1551-2916.2009.03055.x.
- [84] M.A. Raza, A. Westwood, A. Brown, N. Hondow, C. Stirling, Characterisation of graphite nanoplatelets and the physical properties of graphite nanoplatelet/silicone composites for thermal interface applications, *Carbon*. 49 (2011) 4269–4279.
doi:10.1016/j.carbon.2011.06.002.
- [85] B.Z. Jang, A. Zhamu, Processing of nanographene platelets (NGPs) and NGP nanocomposites: A review, *Journal of Materials Science*. 43 (2008) 5092–5101.
doi:10.1007/s10853-008-2755-2.
- [86] I. Erukhimovich, M.O. de la Cruz, Phase equilibria and charge fractionation in polydisperse polyelectrolyte solutions, *Published Online in Wiley InterScience*. (2004) 888–897. doi:10.1002/polb.
- [87] W. Khaliq, V. Kodur, High temperature mechanical properties of high-strength fly ash concrete with and without fibers, *ACI Materials Journal*. 109 (2012) 665–674.
doi:10.14359/51684164.
- [88] J. Du, Y. Li, X. Zheng, Effect of nano-graphite on friction performance of Cu-based friction material, in: *Advanced Materials Research*, 2011: pp. 905–908.
doi:10.4028/www.scientific.net/AMR.284-286.905.
- [89] A. C150/C150M, Standard Specification for Portlan cement, C150/C150M, ASTM. (2018) 1–9. doi:10.1520/C0150.
- [90] ACI, American Concrete Institute (ACI), Report on High-Strength Concrete, ACI 363R-10, American Concrete Institute, Detroit, MI, USA., 2010.
- [91] ASTM C192, Standard practice for making and curing concrete test specimens in the Laboratory, (2003) 1–15. doi:10.1520/C0192.
- [92] ASTM C39, Standard Test Method for Compressive Strength of Cylindrical Concrete Specimens, American Society for Testing and Materials. (2016) 1–7.

- doi:10.1520/C0039.
- [93] ASTM International, ASTM C496 Standard Test Method for Splitting Tensile Strength of Cylindrical Concrete Specimens, ASTM International. (2011) 5.
doi:10.1520/C0496.
- [94] W. Khaliq, H.A. Khan, High temperature material properties of calcium aluminate cement concrete, *Construction and Building Materials*. 94 (2015) 475–487.
doi:10.1016/j.conbuildmat.2015.07.023.
- [95] R.D. Recommendation, P.D.E. Recommendation, D.E.L.A. Rilem, C. At, H. Temperatures, Rilem draft recommendation 129-MHT test methods for mechanical properties of concrete at high temperatures compressive strength for service and accident conditions, (1996) 410–414.
- [96] RILEM TC 129-MHT: Test methods for mechanical properties of concrete at high temperatures Recommendations Part 4 : Tensile strength for service and accident conditions, 33 (2000) 219–223.
- [97] ASTM Standard C469/C469M, Standard Test Method for Static Modulus of Elasticity and Poisson's Ratio of Concrete in Compression, ASTM International. (2014) 1–5.
doi:10.1520/C0469.
- [98] ASTM International, ASTM C597 Standard Test Method for Pulse Velocity Through Concrete, 2016. doi:10.1520/C0597-16.2.
- [99] Y. Fu, L. Li, Study on mechanism of thermal spalling in concrete exposed to elevated temperatures, *Materials and Structures/Materiaux et Constructions*. 44 (2011) 361–376. doi:10.1617/s11527-010-9632-6.
- [100] M. Karevan, K. Kalaitzidou, Understanding the property enhancement mechanism in exfoliated graphite nanoplatelets reinforced polymer nanocomposites, *Composite Interfaces*. 20 (2013) 255–268. doi:10.1080/15685543.2013.795752.
- [101] M. Li, C.X. Qian, W. Sun, Mechanical properties of high-strength concrete after fire, *Cement and Concrete Research*. 34 (2004) 1001–1005.
doi:10.1016/j.cemconres.2003.11.007.
- [102] . B., STUDY OF MECHANICAL PROPERTIES OF CONCRETE AT ELEVATED TEMPERATURES - A REVIEW, *International Journal of Research in Engineering and Technology*. 02 (2013) 317–330. doi:10.15623/ijret.2013.0208050.

- [103] T. Gupta, S. Siddique, R.K. Sharma, S. Chaudhary, Effect of elevated temperature and cooling regimes on mechanical and durability properties of concrete containing waste rubber fiber, *Construction and Building Materials*. 137 (2017) 35–45.
doi:10.1016/j.conbuildmat.2017.01.065.
- [104] F.P. Cheng, V.K.R. Kodur, T.C. Wang, Stress-strain curves for high strength concrete at elevated temperatures, *Journal of Materials in Civil Engineering*. 16 (2004) 84–90.
doi:10.1061/(ASCE)0899-1561(2004)16:1(84).
- [105] W. Khaliq, V. Kodur, Thermal and mechanical properties of fiber reinforced high performance self-consolidating concrete at elevated temperatures, *Cement and Concrete Research*. 41 (2011) 1112–1122. doi:10.1016/j.cemconres.2011.06.012.
- [106] B. Han, S. Sun, S. Ding, L. Zhang, X. Yu, J. Ou, Review of nanocarbon-engineered multifunctional cementitious composites, *Composites Part A: Applied Science and Manufacturing*. 70 (2015) 69–81. doi:10.1016/j.compositesa.2014.12.002.
- [107] ASTM International, ASTM C597 Standard Test Method for Pulse Velocity Through Concrete, ASTM International. (2016) 4. doi:10.1520/C0597-16.2.
- [108] R.A. Khushnood, A. Nawaz, Effect of adding graphite nano/micro platelets on salt freeze-thaw resistance of nano-modificent concrete, *Materials Research Express*. 6 (2019) 095023. doi:10.1088/2053-1591/ab2d86.
- [109] Minitab. Minitab Inc, (2018). <http://www.minitab.com/en-us/products/minitab/>.2018.